Andreas Aufschnaiter, BSc.

Impact of vacuolar function on alpha-synuclein cytotoxicity in a yeast model of Parkinson's disease

MASTER'S THESIS

to achieve the university degree of

Master of Science

Master's degree programme: Biochemistry and Molecular Biomedical Sciences

submitted to

Graz University of Technology

Supervisor

Priv. Doz. Dr. Sabrina Büttner

Institute of Molecular Biosciences
University of Graz

Graz, June 2015

AFFIDAVIT

I declare that I have authored this thesis independently, that I have not used other than the declared sources/resources, and that I have explicitly indicated all material which has been quoted either literally or by content from the sources used. The text document uploaded to TUGRAZonline is identical to the present master's thesis dissertation.

25. June. 2015
Date

Signature

Content

1. Introduction

Parkinson's disease (PD) is the second most common neurodegenerative disease worldwide. It is characterised by cell death of dopaminergic neurons in the substantia nigra pars compacta, a structure in the brain crucial for controlling movement. This leads to motor symptoms like tremor, rigidity and bradykinesia, however a wide range of non-motor symptoms also occur in later stages of this disease, including autonomic, cognitive and psychiatric disorders.

1.1. Parkinson's disease pathology

Nearly 200 years after the first description of the "shaking palsy" by James Parkinson, the exact mechanisms of the processes leading to neurodegeneration in PD are still mostly unknown. Because of its different aetiologies, PD can be classified in several groups, whereby in the first and most common group, the cause of the disease is unknown. Such cases are called idiopathic Parkinson syndrome or Morbus Parkinson. A second subtype of PD is the familial Parkinson syndrome. As the name implies, patients out of this group descend from families with a higher incidence of PD. Especially this group provided very important insights into the molecular mechanisms underlying PD. A third aetiological group is the symptomatic, or secondary Parkinson syndrome. Patients from this group show Parkinsonism in the context of a metabolic, inflammatory or vascular disease. Further reasons are traumatic injury, intoxication or another neurodegenerative disease (then referred to as atypical Parkinson syndrome). Many risk factors have been described for PD, including pesticide exposure and Beta-blocker use. However, age seems to be the major risk factor. The use of calcium channel blockers and drinking coffee was reported to somehow lower the risk for developing PD [1, 2].

One common feature of the PD groups described above is the degeneration of dopaminergic neurons in the substantia nigra pars compacta, which can be seen macroscopically as depigmentation. The microscopic hallmarks of PD are the so-called Lewy bodies, proteinaceous deposits within neurons that mainly consist of aggregated α-synuclein [3-5].

1.2. α-synuclein in Parkinson's disease

α-synuclein is encoded by the SNCA gene on chromosome 4q21 and has a length of 140 amino acids. Its physiological role is not fully understood yet, but there is evidence that this protein, which abundantly appears in presynaptic terminals, promotes SNARE-complex assembling [5]. α-synuclein consists of three different domains: Several repeats with the consensus sequence KTKEGV are located at the N-terminus. This domain is particularly interesting, since it can contain the three point mutations A30P, E46K and A53T, which are known to be a genetic risk factor for PD [6-8]. The non-amyloid component (NAC) is the second region, followed by the acidic C-terminus as the third domain. In addition to the described point mutations, a genomic multiplication of the SNCA gene can be a cause of PD [9, 10].

α-synuclein is natively unfolded due to its low hydrophobicity and high net charge. Since these two parameters are changed by alterations of pH value and temperature respectively, α-synuclein showed a higher order at pH 3.0 and at high temperature, which leads to aggregation [11].

Other important factors for α-synuclein aggregation are several posttranslational modifications, including phosphorylation, nitration, ubiquitination, and C-terminal truncation. These modifications either promote or inhibit the formation of oligomers and fibrils, depending on the residue where they occur. A few of these modifications will be discussed below to show the complexity of intracellular signalling leading to α-synuclein aggregation and formation of Lewy bodies.

One of the major posttranslational modifications of α-synuclein is the phosphorylation of Ser-129. About 90% of α-synuclein in Lewy Bodies is phosphorylated at this site [12]. This modification was shown to enhance the aggregation properties of α-synuclein, whereas phosphorylation of Ser-87 blocked aggregation in vitro [13, 14].

Ubiquitination is a process involved in protein degradation by marking proteins for the proteolytic breakdown via the proteasome. It was shown that monoubiquitination of Lys-6 through the ubiquitin ligase parkin reduced α-synuclein aggregation [15]. A further common modification of α-synuclein is C-terminal truncation, which is reinforced by the A53T and A30P mutation of α-synuclein [16]. Interestingly, truncation products can interact with full-length α-synuclein to enhance its aggregation and toxic effects [17].

A huge number of modifications and interactions with other Parkinson related proteins are known to influence the aggregation processes of α-synuclein (as reviewed in [18]. These complex mechanisms are far from being completely understood. A further unanswered question in PD pathology is how these aggregates impair cellular integrity, ultimately leading to cell death. Three general mechanisms are therefore discussed. The first explains toxicity through a disruption of cellular compartments. This is indicated by the observation that α-synuclein can bind to lipid membranes and disrupt membrane bilayers [19, 20]. Other models explain α-synuclein toxicity via a toxic gain and loss of function, respectively. High levels of α-synuclein or pathological point mutants result in an impairment of vesicle trafficking, (especially ER-to-Golgi complex trafficking) [21], mitochondrial defects and oxidative stress [22], deficiency in proteasomal degradation [23], imbalance of Ca^{2+} homeostasis [24] and insufficient autophagy [25].

1.3. Autophagy: a matter of life and death

Deposits of misfolded and aggregated proteins are a common feature of many neurodegenerative diseases. Actually, some of these diseases can be classified by the kind of protein that accumulates in specific regions in the brain. For example, Alzheimer's disease and Morbus Pick belong to a group called tauopathies, named after the pathologically aggregated tau protein. Diseases with α-synuclein containing deposits are named synucleinopathies, including dementia with Lewy bodies, multiple system atrophy and PD. Protein aggregation being a major cause for neurodegeneration makes it quite obvious that autophagy is linked to these diseases, since it is involved in the degradation of dysfunctional cellular components.

Autophagy can be broadly divided into three main types, namely chaperone-mediated autophagy, microautophagy and macroautophagy. Chaperone-mediated autophagy is a process only occurring in higher eukaryotes (so far not known for yeast), in which proteins are unfolded by chaperones and then transported to the lysosomal membrane [26]. In microautophagy, cytosolic elements are directly taken up via invagination or protrusion of the lysosome [27]. Macroautophagy is characterized by the formation of double-membrane vesicles, called autophagosomes, which sequester unused or damaged substrates in order to transport them to the lysosome [28]. Macroautophagy (hereafter called autophagy) is the main mechanism to degrade long-lived proteins like α-synuclein. Furthermore, it is the only mechanism for degrading whole organelles, like damaged mitochondria, which have an important role in PD [22].

Evidence for the involvement of autophagy in PD came from postmortem brain analysis, where an accumulation of autophagosomes in neuronal tissue was observed [29]. Furthermore, an activation of autophagy by overexpression of beclin 1, led to a reduction of α-synuclein aggregation [30]. Most studies showed neuroprotective effects of autophagy in PD models [31-34]. Still in distinct cellular scenarios, the induction of autophagy turned out to have rather negative effects on α-synuclein-mediated toxicity [35, 36]. This controversy highlights the importance of well-balanced autophagic processes to maintain cell integrity.

1.3.1. Calcium signalling in autophagy and Parkinson's disease

Calcium is an important second messenger and therefore essential in a wide range of signal transduction processes, like regulation of enzymatic activities, permeability of ion channels, regulation of cytoskeleton dynamics, but also in autophagy and apoptosis. Furthermore, a wide range of neurophysiological processes depends on Ca^{2+}, including synaptic plasticity in learning and memory formation [37, 38] as well as neuronal cell death in processes like excitotoxicity [39]. The fact that Ca^{2+} is involved in the formation of new synaptic connections, but also in neuronal cell death, indicates the crucial role of a precisely balanced Ca^{2+} homeostasis, which needs a sophisticated regulation system.

In addition, Ca^{2+} is involved in apoptosis and here again it can function as a pro- as well as an anti-apoptotic signal [40]. In PD, Ca^{2+} homeostasis and cell death seem connected, as suggested by the finding that α-synuclein alters cellular and in particular cytosolic Ca^{2+} levels [24, 41]. Moreover, direct interaction of Ca^{2+} with the C-terminus of α-synuclein enhanced the aggregation process [42], pointing out a crucial role of Ca^{2+} homeostasis in PD.

1.3.2. Lysosomal breakdown – the weakest link in protein clearance?

The last step in autophagy is the lysosomal breakdown, in which the unused or damaged substrate is degraded by acidic hydrolases. Since the accumulation of autophagosomes, observed in postmortem brains, is not necessarily a sign for an up-regulation of autophagy, but can also indicate a problem of the autophagosomal clearance, the autophagosome-lysosome fusion and the vacuolar breakdown might be particularly interesting in PD. Indeed, there are studies, suggesting a pathogenic lysosomal depletion in PD [43], which might be caused by the production of reactive oxygen species (ROS), followed by lysosomal membrane permeabilization (LMP) and the release of acid proteases like Cathepsin D into the cytosol [44].

1.3.3. Possible role of Cathepsin D in Parkinson's disease

Cathepsin D is a human lysosomal aspartyl protease with various physiological functions, ranging from degradation of intracellular proteins and polypeptide hormones to the activation of hormones, growth factors, enzymatic precursors and the regulation of programmed cell death. Beside its physiological functions, Cathepsin D was linked to pathophysiological processes, especially in cancer [45].

The yeast counterpart of this protein is Pep4p (or proteinase A), which is synthesized as a 405 amino acid long zymogen. After its glycosylation in the endoplasmatic reticulum, the propeptide with a length of 54 amino acids is cleaved within the vacuole, where Pep4p complies its function as vacuolar aspartyl protease, which is important for autophagic protein breakdown [46].

Pep4p overexpression was shown to enhance the chronological lifespan of yeast cells, which was not due to its protease activity, since a double point mutation of Pep4p, completely lacking its enzymatic activity, showed similar effects. Further, even the overexpression of the propeptide of Pep4p had pro-survival effects. This study indicated an anti-apoptotic and anti-necrotic function of Pep4p [47].

Recent studies observed lower α-synuclein aggregation properties and toxicity levels in neuronal cell culture, *Drosophila melanogaster* and *Caenorhabditis elegans* models when Cathepsin D was overexpressed, linking this proteinase to the pathological changes in PD [48, 49]. Inconsistent with these results, another study reported an enhanced α-synuclein aggregation caused by Cathepsin D, which seemed to cause C-terminal truncation, a process involved in α-synuclein aggregation [50]. Therefore, the role of Cathepsin D in PD remains enigmatic.

1.4. Humanized yeast models to study Parkinson's disease

One of the main problems in PD research is not just the complexity of the pathological changes in affected cells, but also the per se very sophisticated physiology of neurons. This was the reason for a new approach performed nearly a decade ago: Instead of using model organisms like *Drosophila melanogaster* or *Caenorhabditis elegans* with a quite simple nervous system, scientists used a model that completely lacks neurons but shares important basic molecular mechanisms affected in neurodegeneration like protein folding, quality control and degradation, autophagy, apoptosis and the mitochondrial respiratory chain. This was the birth of the budding yeast *Saccharomyces cerevisiae* as a model for studying neurodegenerative disease [51].

As eukaryotic, but single-celled organism, yeast is very easy to handle and can be genetically modified with simple methods. This allows high throughput screens to gain new insights into pathophysiological conditions of several neurodegenerative diseases.

Humanized yeast models for PD were designed by heterologous expression of human α-synuclein. Since yeast lacks counterparts of human PD-associated proteins, these models allow the selective study of certain factors in α-synuclein pathophysiology. α-synuclein expressing yeast was sufficient to reflect established data from higher models, like growth inhibition, oxidative stress, mitochondrial dysfunction, cell death, aggregation and dysfunctions in apoptosis [22, 51, 52]. In addition, also new insights in PD pathology were initially gained by using yeast models, like the impairment of vesicular trafficking [21].

This study used a yeast model of PD, heterologously expressing human α-synuclein. In this model, the yeast ortholog of Cathepsin D, Pep4p, was overexpressed to investigate its controversially discussed impact on α-synuclein pathophysiology. Furthermore, connections between autophagy, Ca^{2+} homeostasis and changes of cell physiology through Pep4p and α-synuclein overexpression were determined to identify new potential pathways in PD pathology.

2. Material and methods

2.1. Yeast strains and plasmids

Experiments were carried out in BY4741 (MAT a; his3Δ1; leu2Δ0; met15Δ0; ura3Δ0) and respective null mutants, obtained from Euroscarf. To monitor Ca^{2+}/Pep4p connection the Pep4p-knockout strain BY4741 (Mat a; his3Δ1; leu2Δ0; met15Δ0; ura3Δ0; YMR174c::kanMX4) from Euroscarf was used. For investigation of autophagy, a previously published [53] endogenous GFP-tagged Atg8p expressing strain was used (BY4741 pATG8::natNT2-pATG8-EGFP).

Strains used for overexpression of FLAG-tagged wild type Pep4p ($Pep4p^{WT}$), double point mutation (D109A, D294A) of Pep4p ($Pep4p^{DPM}$) and the propeptide of Pep4p ($Pep4p^{Pro}$) were created by yeast-transformation using a $pESC_{-his}$ vector (Stratagene, Agilent Technologies, Vienna, Austria). These plasmids were kindly provided by Didac Carmona-Gutierrez [47]. For heterologous expression of C-terminal FLAG-tagged human α-synuclein a $pESC_{-ura}$ vector was used. Therefore, previously published α-syn-$pESC_{-his}$ constructs [22] were cut with *SpeI* and *ClaI* and ligated into $pESC_{-ura}$.

2.2. Growth media

Yeast strains were grown either on full media (YPD), or synthetic medium (SM). YPD consisted of 1% yeast extract (Bacto, BD Biosciences, Schwechat, Austria), 2% peptone (Bacto, BD Biosciences, Schwechat, Austria) and 4% D-glucose. For clonogenic survival experiments, cells were plated on YPGly plates, containing 1% yeast extract (Bacto, BD Biosciences, Schwechat, Austria), 2% peptone (Bacto, BD Biosciences, Schwechat, Austria) and 3% glycerol.

SM contained 0.17% yeast nitrogen base (Difco, BD Biosciences, Schwechat, Austria), 0.5% $(NH_4)_2SO_4$ and 30 mg/L of all amino acids (except 80 mg/L histidine and 200 mg/L leucine), 30 mg/L adenine and 320 mg/L uracil with 2% D-glucose (SMD) or 2% D-galactose (SMG).

Escherichia coli (E. coli) XL-1 were grown on LB medium containing 0.5% yeast extract (Bacto, BD Biosciences, Schwechat, Austria), 1% tryptone (Bacto, BD Biosciences, Schwechat, Austria) and 0.5% NaCl. 1 µg/mL ampicillin was added for selection when required (LB-AMP).

All media were prepared with double distilled water and subsequently autoclaved (25 min, 121°C, 210 kPa). Amino acid mixtures were sterilized separately as 10x stocks and added after autoclaving. For solid media 2% agar was admixed.

2.3. Solutions and buffers

The composition of used solutions and buffers can be seen in Table 1.

Table 1: Composition of solutions and buffers used in this study.

Solution	Composition
Yeast transformation	
10x TE	100 mM Tris in ddH_2O; pH 8.0 10 mM EDTA
10x LiAc	1 M LiAc in ddH_2O
50%PEG 4000	50% Polyethylene glycol 4000 in ddH_2O
ssDNA	Salmon sperm DNA (10 mg/mL)
DNA electrophoresis	
Agarose-gel	80 mM Tris-HCl; pH 8.0 0.2 M EDTA Ethidium bromide 1% Agarose
Running buffer	80 mM Tris-HCl; pH 8.0
Cryostocks	50% Glycerol
FACS	
PBS	25 mM potassium phosphate; pH 7.0 0.9% NaCl
DHE	Stock solution (2.5 mg/mL) 1:1000 diluted in PBS
PI	Stock solution (1.6 mg/mL) 1:500 diluted in PBS

Microscopy	
MDY-64/PI co-staining	Staining solution: 10 mM HEPES; pH 7.6 5% D-glucose MDY-64 in ddH_2O Wash solution: 10 mM HEPES; pH 7.6 5% D-glucose PI in ddH_2O
Quinacrine/PI co-staining	Solution 1: 100 mM HEPES; pH 7.6 solved in YPD medium Solution 2: 100 mM HEPES; pH 7.6 400 µM Quinacrine solved in YPD medium Solution 3: 100 mM HEPES; pH 7.6 2% D-glucose in ddH_2O Solution 4: 100 mM HEPES; pH 7.6 2% D-glucose 3.2 µg/mL PI in ddH_2O
LMP Assay	Fluorescein isothiocyanate-dextran, Sigma-Aldrich With average molecular weight of 10, 40, 70, 250 kDa each 5 mg/mL in SMD media
Pep4p enzymatic activity assay	Cathepsin D Assay Kit, Sigma-Aldrich (CS0800 Sigma)

SDS-Page and Immunoblot	
Urea loading buffer	200 mM Tris-HCl; pH 6.8 8 M urea 5% SDS 1 mM EDTA 0.02% bromphenol blue 15 mM DTT DHE
6x Lämmli buffer	50 mM Tris-HCl; pH 6.8 2% SDS 10% glycerol 0.1% bromphenol blue 100 mM 2-mercaptoethanol
Electrophoresis buffer	25 mM Tris-HCl; pH 8.3 190 mM glycine 0.2% SDS
Stacking gel	250 mM Tris-HCl; pH 6.8 1% SDS 5 % acrylamide 0.13% N,N'-methylenebisacrylamide 0.1 % ammonium peroxodisulfate 0.01% tetramethylethylenediamine
Separating gel	250 mM Tris-HCl; pH 8.8 0.2% SDS 12.5% acrylamide 0.4% N,N'-methylenebisacrylamide 0.1 % ammonium peroxodisulfate 0.01% tetramethylethylenediamine
Stacking gel seminative	250 mM Tris-HCl; pH 6.8 5 % acrylamide 0.13% N,N'-methylenebisacrylamide 0.1 % ammonium peroxodisulfate 0.01% tetramethylethylenediamine
Separating gel seminative	250 mM Tris-HCl; pH 8.8 10% acrylamide 0.4% N,N'-methylenebisacrylamide 0.1 % ammonium peroxodisulfate 0.01% tetramethylethylenediamine

Blotting buffer	10 mM CAPS; pH 11.0 10% methanol in ddH_2O
TBS(-T)	10 mM Tris-HCl; pH 7.6 150 mM NaCl (0.02% Triton-X-100)
Blocking solution	1% milk powder in TBS
CASY™ Cell Counter	
CASYton	0.9 mM NaCl 0.1 mM EDTA

2.4. *Escherichia coli* transformation

Plasmids were transformed by electroporation in *Escherichia coli* (*E. coli*) *XL-1* cells, in order to amplify constructs for yeast transformation. All ingredients were kept on ice during the whole procedure. 1 µL of plasmid DNA (~ 1 ng DNA) was added to 40 µL of competent *E.coli XL-1* cells and transferred into a sterile electroporation cuvette. By tapping the cuvette, the mixture settled to the bottom and residual water (cuvettes kept on ice) on the outside of the cuvette was removed. The sample was pulsed using a Multiporator 2510 (Eppendorf) adjusted to 2500 V (25kV/cm field strength). Immediately after electroporation, 1000 µL LB medium (without ampicillin) was added and cells were transferred into a new sterile reaction tube. Samples were then incubated 45 min at 37°C. Afterwards, 70 µL of the solution were plated on LB-AMP agar plates and incubated at 37°C. After one day at least 4 clones were picked and streaked on LB-AMP plates. After another day of incubation at 37°C, clones were picked for over night cultures (ONCs) in LB-AMP media and were incubated at least for 8 hours at 37°C and 145 rpm. These cultures were then used for cryostocks and for plasmid isolation.

2.5. Plasmid isolation

For plasmid isolation from *E.coli XL-1* Gene JET Plasmid MiniprepKIT (Thermo Scientific) was used. Aberrantly from the KITs included protocol, plasmids were eluted in 30 µL Aqua bidestillata sterilis “Fresenius” (Fresenius, Graz, Austria) in the last step. Plasmid concentration was determined using a NanoDrop ND-1000 Spectrophotometer (PEQLAB Biotechnologies).

2.6. Yeast transformation

Plasmids were transformed into yeast with the lithium acetate method [54]. Therefore, yeast cells were grown in 5 mL of appropriate medium in 50 mL Erlenmeyer flasks at 28°C and 145 rpm over night. After 16-20 hours of growth, the culture was diluted to OD_{600} 0.2 in 50 mL of the same medium (in 250 mL Erlenmeyer flasks) and incubated at 28°C and 145 rpm until OD_{600} 0.6-0.8. The culture was then transferred into a sterile tube and centrifuged for 4 min at 3500 rpm at room temperature. Cells were washed in 10 mL of ddH_2O, centrifuged and resuspended in 10 mL of a 1xLiAc/0.5xTE solution. After another centrifugation step, cells were resuspended in 500 µL of the same solution and incubated for 30 min at 28°C. ssDNA was prepared by heating 10 min at 95°C and afterwards placed on ice for 10 min (cold shock). 5 µL of ssDNA were filled into a sterile reaction tube and ~2 µg Plasmid DNA was added. Next, 50 µL of cell solution were pipetted into the same tube, and 300 µL of reaction mix, consisting of 40% PEG/0.1 M LiAc/1xTE was admixed. Tubes were then vortexed for at least 30 sec and incubated for 30 min at 28°C. After a heat shock at 42°C for 20 min. samples were spun down for 15 sec. and the pellet was resuspended in 70 µL of ddH_2O. The whole solution was platted on SMD-agar plates and incubated at 28°C for 2 days. At least 4 different clones were then picked and streaked on SMD plates. After another two days of incubation at 28°C, clones were picked for ONCs in SMD media (16-20 hours, 28°C, 145 rpm). These cultures were then used for experiments and production of cryostocks.

2.7. Cryostocks

Cryostocks of *E.coli* and yeast strains were performed by adding 500 µL of an ONC in appropriate medium to 500 µL of a sterile 50% glycerol solution in a microcentrifuge tube. Tubes were stored at -80°C.

2.8. Yeast culture conditions

Early-aging experiments were performed using ONCs which were grown in eprouvettes, using 2 mL SMD for 16-20 hours at 28°C and 145 rpm. These cultures were inoculated in 10 mL SMD (in 100 mL Erlenmeyer flasks) to OD_{600} 0.1 and grown to OD_{600} 0.3. After that cells were transferred into 96-Well deep well plates (VWR, Radnor, USA) with a Matrix electronic multichannel pipette (Thermo Scientific, New Hampshire, USA), whereat 500 µL of cell culture per well was used. Plates were centrifuged for 5 min at 4000 rpm and supernatant was removed. Cells were then resuspended in 500 µL SMG per well for induction of expression. In every experiments a minimum of three different clones were tested, whereupon all of these clones were examined in four different wells. In this manner at least a twelve-fold determination was performed.

2.9. Analysis of *S. cerevisiae* cell death and oxidative stress

2.9.1. Clonogenicity assay

Samples from aged cultures were diluted 1:100 in ddH_2O and the number of cells was measured using a CASY™ cell counter by a further 1:100 dilution in 1xCASYton. Subsequently, the 1:100 diluted samples from aged cultures were adjusted to a final dilution of 1:10000 in ddH_2O and the volume corresponding to 500 cells (both viable and dead) was plated on YPD plates. Plates were incubated for 2 days at 28°C and the number of formed colonies were determined. Survival was defined as the ability to form colonies.

2.9.2. Propidium iodide staining

For analysing cell death, $2*10^7$ cells were harvested in 96 well plates with transparent U-bottom. Therefore, cells were centrifuged for 5 min at 3500 rpm. Cells were resuspended in 250 µL PBS containing 100 ng/mL propidium iodide (PI) and incubated for 10 minutes in the dark. After a further centrifugation step, cells were resuspended in 250 µL PBS and quantification of PI-positive cells was done by flow cytometry (FACSAria, BD Biosciences, Schwechat, Austria). At each time point 30,000 cells were evaluated per well with FACSDivia software.

2.9.3. Dihydroethidium staining

For quantification of produced ROS, the same setup as used for PI staining was performed with dihydroethidium (DHE) staining. Therefore, 2.5 µg/mL DHE were admixed in 250 µL PBS per well.

2.10. Chemical lysis

For expression control using immunoblots, cells with OD_{600} 3.0 were harvested from aged cultures, 24 hours after induction and centrifuged for 1 min at 10,000 rpm. Then, pellets were resuspended in 150 µL lysis buffer CP and incubated for 10 min on ice. After that 150 µL 4°C cold TCA (55%) were added and incubated another 10 min on ice. Lysates were then centrifuged for 10 min at 10,000 rpm and the supernatant was removed. The pellet was carefully resuspended in 150 µL of urea loading buffer and 1M Tris was added in 5 µL steps, until the suspension turned blue. Samples were then incubated for 5 min at 65°C.

For showing aggregates of α-synuclein, lysis and immunoblotting was performed using a “semi-native approach”. Therefore, cells with OD_{600} 8.0 were harvested from aged cultures, 24 hours after induction and centrifuged for 1 min at 10,000 rpm. Pellets were resuspended in 200 µL of 0.1 M NaOH and shaken for 5 min at 1400 rpm and 21°C. Samples were then centrifuged for 5 min at 4000 rpm and supernatant was discarded. Then, pellets were resuspended in 150 µL of 1xLämmli buffer and once again shaken for 5 min at 1400 rpm, 21°C. After that samples were centrifuged for 1 min at 14,000 rpm and supernatant was used for gel electrophoresis.

2.11. SDS-PAGE and immunoblotting

For expression controls, 15 µL of the lysate were loaded on a 12.5% polyacrylamide gel. Gels were run at 12 mA per gel, until the sample reached the separating gel. Then current was adjusted to 16 mA per gel. As a standard, 2.5 µL of PageRuler™ prestained protein ladder (Thermo Scientific) were used.

Proteins were transferred to a PVDF membrane (Millipore) in a blotting chamber filled with Blotting buffer at 220 mA for 60 min. Membranes were washed with TBS and then blocked with blocking solution for 60 min. Afterwards, membranes were washed with TBS-T for 5 min. 10 mL of the primary antibody were added per membrane and incubated over night at 4°C. The next day, membranes were washed three times with TBS-T for 5 min each and the secondary antibody was incubated for 60 min at room temperature. After four washing steps with TBS-T for 5 min, 1.5 mL of the ECL detection solution was thoroughly distributed on each membrane and incubated for 1 min. Membranes were then detected using a Bio-Rad ChemiDoc™ Touch Imaging System (Bio-Rad Laboratories Ges.m.b.H, Vienna, Austria).

The same setup was used for detection of α-synuclein aggregates, whereby 18 µL of protein solution were loaded on 10% polyacrylamide semi-native gels (without SDS). All steps were carried out in a cold-room at 4°C.

2.12. Fluorescence microscopy

Different stainings used in this work are described below. In every experiment observation was done with a Zeiss Axioskop microscope (Zeiss, Vienna, Austria).

2.12.1. Quinacrine/PI staining

$1*10^8$ cells from aged cultures, 24 hours after induction, were harvested in reaction tubes and washed with 500 µL of solution 1. Samples were centrifuged for 1 min at 13,000 rpm (parameters used in every centrifugation step) and the pellet was resuspended in 500 µL of solution 2 (contained Quinacrine). After an incubation for 10 min at 28°C and 145 rpm, samples were incubated 5 min on ice. Then, cells were centrifuged and washed twice in 500 µL cold solution 3. For the PI co-staining, 500 µL of solution 4 was added and incubated 10 min in the dark on ice. Cells were then centrifuged and examined by fluorescence microscopy.

2.12.2. PI and DHE staining

Samples were either gained by pooling cells from 96-well plates after FACS measurement and directly used for microscopy, or $2*10^7$ cells from aged cultures were harvested in reaction tubes and washed with 500 µL PBS. After centrifugation for 1 min at 10,000 rpm the fluorescence dye (100 ng/mL PI or 2.5 µL DHE, each in 500 µL PBS) was added and incubated for 10 min in the dark. After a further centrifugation step, cells were observed with a fluorescence microscope.

2.12.3. Lysosomal membrane permeabilization assay

For detection of lysosomal membrane permeabilization (LMP), $1*10^8$ cells from aged cultures were harvested in reaction tubes and washed with SMD. Fluorescein isothiocyanate-dextrans (Sigma-Aldrich) with average molecular weight of 10 kDa, 40 kDa, 70 kDa and 250 kDa were solved in SMD with a final concentration of 5 mg/mL. 200 µL of these solutions were separately added to the samples. After resuspension, samples were incubated for 60 min at 28°C and 145 rpm. Then, cells were centrifuged for 1 min at 10,000rpm and 4°C.

It was important to keep samples on ice for the further procedure. After washing cells three times with PBS, co-staining with PI as performed to exclude dead cells. Therefore, cells were incubated with 200 µL of PI in PBS (100 ng/mL) for 10 min in the dark at 4°C. Samples were then centrifuged for 1 min at 10,000 rpm, 4°C and examined using a fluorescence microscope.

2.12.4. GFP/PI staining

$1*10^8$ cells with endogenously GFP-tagged Atg8p from aged cultures were harvested in reaction tubes and co-stained with PI to exclude dead cells. This co-staining was done in the same way as for the LMP assay mentioned above.

2.12.5. MDY-64 staining

$1*10^7$ cells from aged cultures were harvested in reaction tubes and washed with 500 µL PBS. After centrifugation for 1 min with 10,000 rpm, pellets were resuspended in 200 µL MDY-64 staining solution and incubated for 20 min in the dark. Cells were then centrifuged and the pellet was washed in the MDY-64 wash solution. PI co-staining was performed as described for the LMP assay.

2.13. Pep4p enzymatic activity assay

To measure the enzymatic activity of Pep4p, a Cathepsin D activity assay kit (fluorometric) from Abcam was used and the protocol was adapted for yeast probes.

2.13.1. Sample collection and cell lysis

$2*10^8$ cells were harvested from aged cultures in reaction tubes and resuspended in chilled CD cell lysis buffer. 100 µL of glass beads were added and vortexed three times for 1 min at 4°C with an incubation time of 1 min between each cycle. Supernatant was transferred into a fresh reaction tube and centrifuged for 5 min at 10,000 rpm. The clear lysate was then transferred into a new reaction tube and kept on ice during the further experimental procedure.

2.13.2. Determination of protein concentration

In a two-fold determination the clear lysate was used to measure the protein concentration via the Bradford assay in a 96 well plate. Therefore 40 µL of the lysate per determination were used. A standard curve with BSA was created by dilution series of a 1 mg/mL stock solution. 250µL of Bradford reagent (Bio-Rad Laboratories Ges.m.b.H, Vienna, Austria) were added per well and incubated for exactly 5 min. The protein concentration was quantified by measurement of the OD_{600} in a Tecan Genios pro microplate reader (Tecan Austria GmbH, Gröding, Austria).

2.13.3. Fluorescence Pep4p activity assay

The volume of lysate corresponding to 0.1 µg protein was pipetted into a 96-well plate with transparent F-bottom and filled with chilled CD cell lysis buffer to a total volume of 50 µL. Then, 52 µL of a master mix (50 µL supplied reaction buffer + 2 µL supplied substrate) were added per well and the plate was incubated for 2 hours at 28°C. To detect the enzymatic activity of Pep4p, the fluorescence (ex: 328 nm, em: 460 nm) was measured using a Tecan Genios pro microplate reader (Tecan Austria GmbH, Gröding, Austria). The enzymatic activity is shown as the mean fluorescence intensity per µg protein.

2.14. Statistics

To disprove the null-hypothesis (no difference between conditions), significance and p-values were calculated by using one-way ANOVA, corrected with a Bonferroni post-hoc test for one variable (type of expression). For two variables (type of expression and time) a two-way ANOVA, corrected by a Tukey post-hoc test was used. Significance is indicated with asterisks: *** $p<0.001$, ** $p<0.01$, * <0.05. Statistics were conducted with IBM SPSS 22 and figures were processed with Microsoft Excel and Microsoft PowerPoint.

3. Results

3.1. α-synuclein cytotoxicity in a yeast model of Parkinson's disease

In this study, a yeast model of PD was used. Heterologous expression of human α-synuclein was achieved using a galactose-inducible promotor, as done in previous studies [22, 24, 55]. Since in this work the expression of α-synuclein was performed using a $pESC_{-ura}$ vector (instead of a $pESC_{-his}$ vector), the toxicity of α-synuclein in this model was re-evaluated using ROS production and cell death.

Cell death was determined via PI staining followed by flow cytometric quantification. This was performed 16, 24 and 48 hours after induction of expression. As shown in Figure 1, α-synuclein significantly increased the number of dead cells throughout the whole expression period.

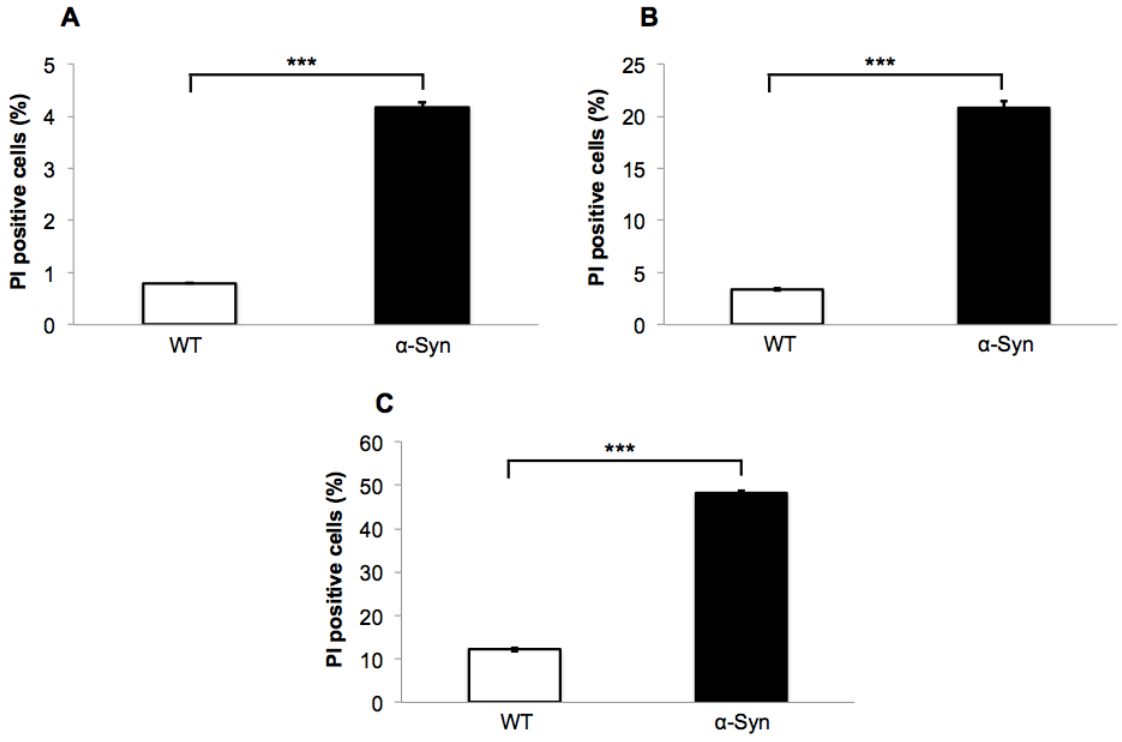

Figure 1: Cell death indicated by flow cytometric quantification of propidium iodide (PI) staining of wild type (WT) cells and cells heterologously expressing α-synuclein (α-Syn). Cell death was analysed 16 h (A), 24 h (B) and 48 h (C) after induction. Means ± s.e.m., n=16. ***P<0.001

To demonstrate production of ROS, cells were stained with DHE, which is converted to fluorescent ethidium via oxidation, and evaluated via flow cytometry. As shown in Figure 2, α-synuclein expressing cells also produced a significant higher amount of ROS compared to WT cells only harbouring the empty vector.

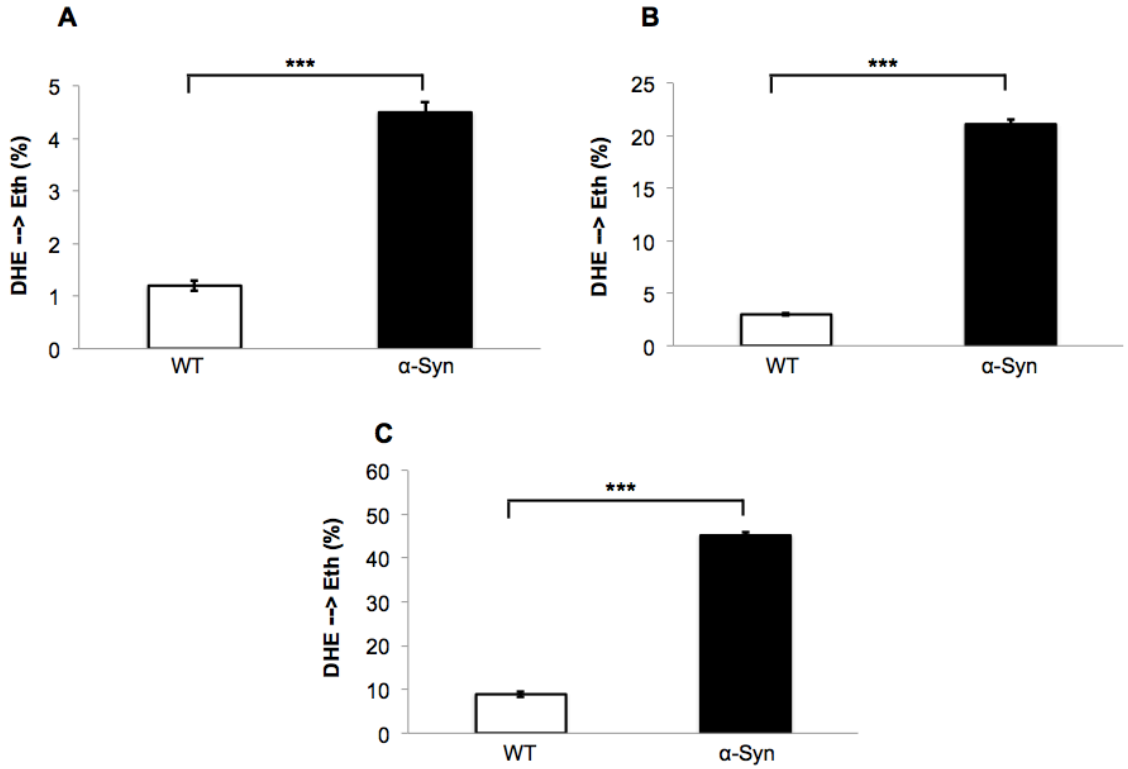

Figure 2: ROS accumulation indicated by flow cytometric quantification of DHE to Eth conversion of wild type cells (WT) and α-synuclein expressing cells (α-Syn). ROS production was analysed 16 h (A), 24 h (B) and 48 h (C) after induction. Means ± s.e.m., n=16. ***P<0.001

Heterologous expression of human α-synuclein in *Saccharomyces cerevisiae* significantly increased ROS production and cell death. The conclusive phenotype of α-synuclein expressing yeast cells confirmed the ability of the constructed model to reflect pathological changes of PD. Already 48 hours after induction a cell death rate of 50% was observed. Thus, this early phase of expression was monitored in further experiments.

3.2. Pep4p overexpression alleviated α-synuclein-caused cell death and ROS production

Since α-synuclein toxicity led to massive cell death in the present yeast model, an early-aging experiment was performed to study the influence of Pep4p variants on this effect. Cell death was analysed 16, 24 and 48 hours after induction via PI staining followed by flow cytometric quantification. As depicted in Figure 3, a clear decrease of α-synuclein toxicity was observed upon co-expression of $Pep4p^{WT}$ after 24 and 48 hours of growth on galactose. Abrogation of the proteolytic activity ($Pep4p^{DPM}$) had no significant influence on α-synuclein toxicity. Interestingly, overexpression of the propeptide of Pep4p ($Pep4p^{PRO}$) led to a significant increase of cell death caused by α-synuclein after 16 hours of expression, while $Pep4p^{WT}$ had no significant effect on α-synuclein toxicity in this early phase of expression. In addition, $Pep4p^{PRO}$ overexpression increased α-synuclein toxicity 24 and 48 hours after induction.

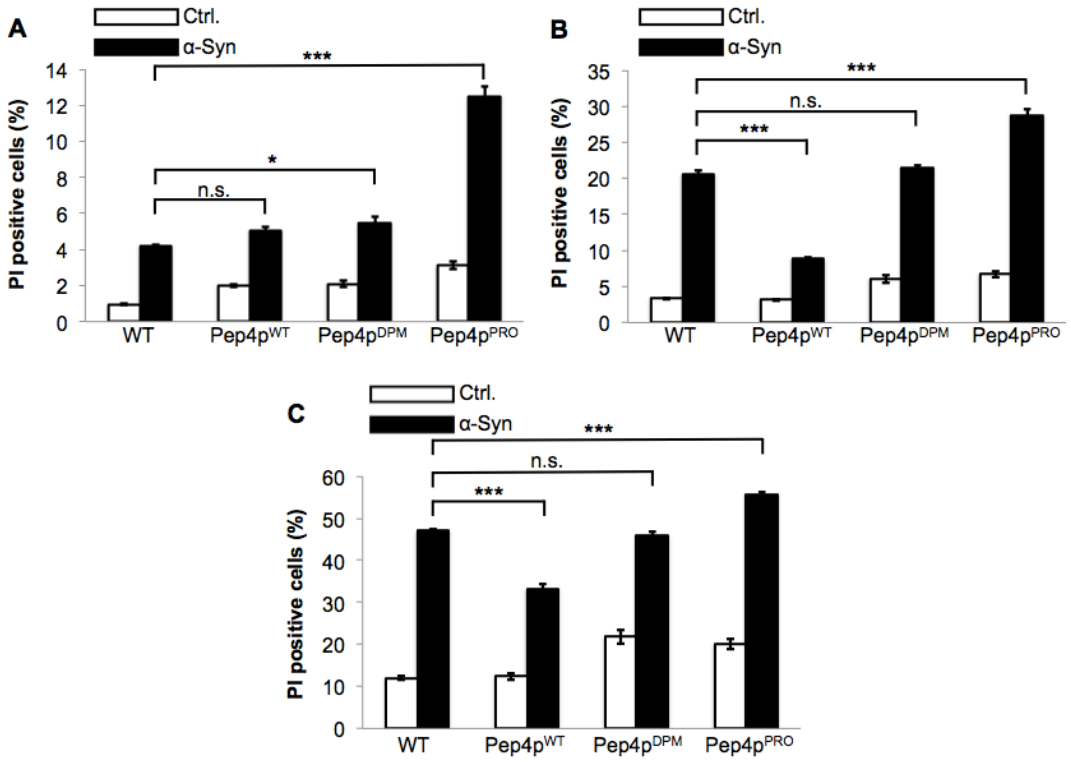

Figure 3: Cell death indicated by flow cytometric quantification of propidium iodide (PI) staining of wild type cells (WT), Pep4p wild type ($Pep4p^{WT}$), double point mutation of Pep4p ($Pep4p^{DPM}$) and propeptide of Pep4p ($Pep4p^{PRO}$) expressing cells, with and without co-expression of human α-synuclein (α-Syn). Cell death was analysed 16 h (A), 24 h (B) and 48 h (C) after induction. Means ± s.e.m., n=12. ***P<0.001; *P<0.05; n.s.P>0.05.

Figure 4 indicates the timeline of cell death in the strains expressing α-synuclein alone or in combination with the different Pep4p variants. PI staining suggested an alleviation of α-synuclein toxicity by Pep4p^{WT} overexpression, which might be due to the proteolytic activity of this enzyme, since the enzymatic inactive double point mutation did not shown significant changes.

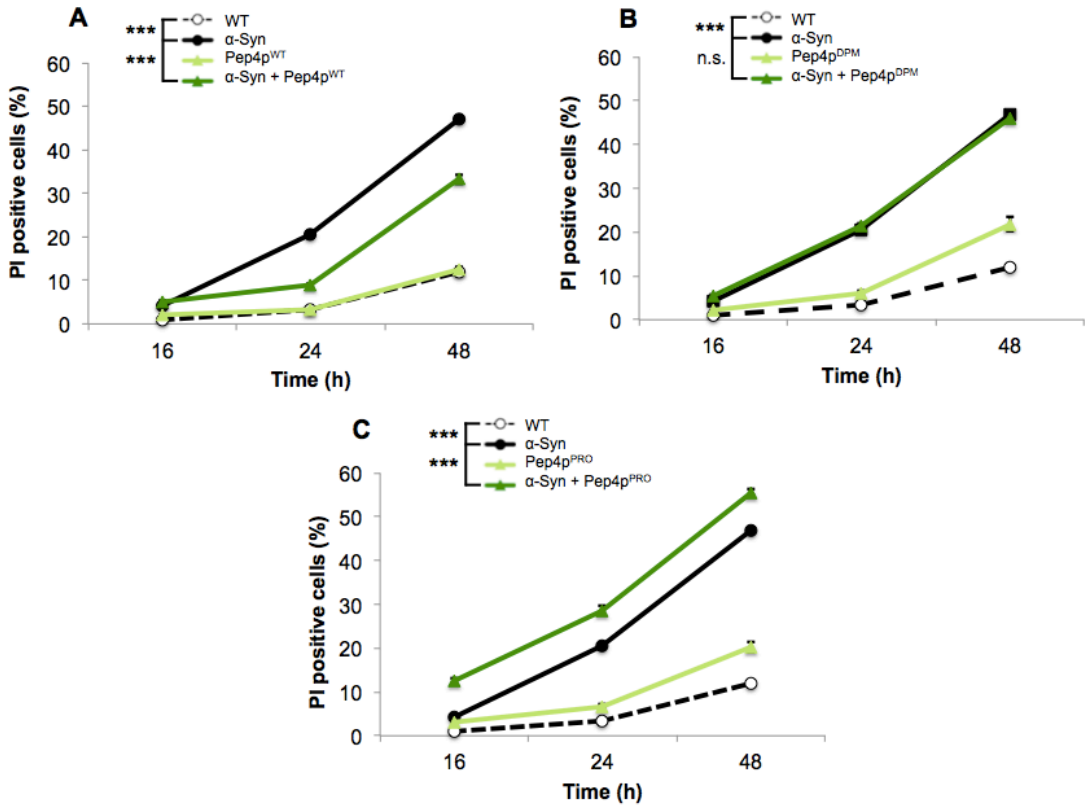

Figure 4: Time course of cell death indicated by flow cytometric quantification of propidium iodide (PI) staining of wild type cells (WT), Pep4p wild type (Pep4p^{WT}), double point mutation of Pep4p (Pep4p^{DPM}) and propeptide of Pep4p (Pep4p^{PRO}) expressing cells, with and without co-expression of human α-synuclein (α-Syn). Cell death was analysed 16 h (A), 24 h (B) and 48 h (C) after induction. Means ± s.e.m., n=12. ***P<0.001; n.s.P>0.05.

To further verify influence of Pep4p^{WT} overexpression on α-synuclein cytotoxicity, a quantification of oxidative stress was performed. Cells were stained after 16, 24 and 48 hours with DHE and quantification of the DHE → Eth conversion was performed by flow cytometry. As shown in Figure 5, α-synuclein caused an increase in oxidative stress compared to the wild type, whereas the overexpression of Pep4p^{WT} diminished this effect. Pep4p^{DPM} showed a higher ROS production 16 hours after induction, but at later time points no significant changes in α-synuclein caused oxidative stress was observed. The even toxicity-fortifying effects of Pep4^{PRO} in term of ROS production were observed throughout the whole experiment.

Figure 6 shows the timeline of ROS production in the different strains. Comparing this data with the time course in Figure 4, a joint appearance of ROS accumulation and cell death caused by α-synuclein is obvious. Further, a reduction of these events by overexpression of Pep4p^{WT} could be observed. To visualize this effect, DHE stained cells were pooled after FACS analysis and analysed by fluorescence microscopy. Figure 7 presents representative pictures of DHE stained cells 24 hours after induction. In these pictures, the reduction of ROS accumulation via Pep4p^{WT} overexpression can be seen as a lower amount of red fluorescing cells. Sample pictures of Pep4p^{DPM} and Pep4p^{PRO} expressing cells can be seen in the supplementary figure S 1.

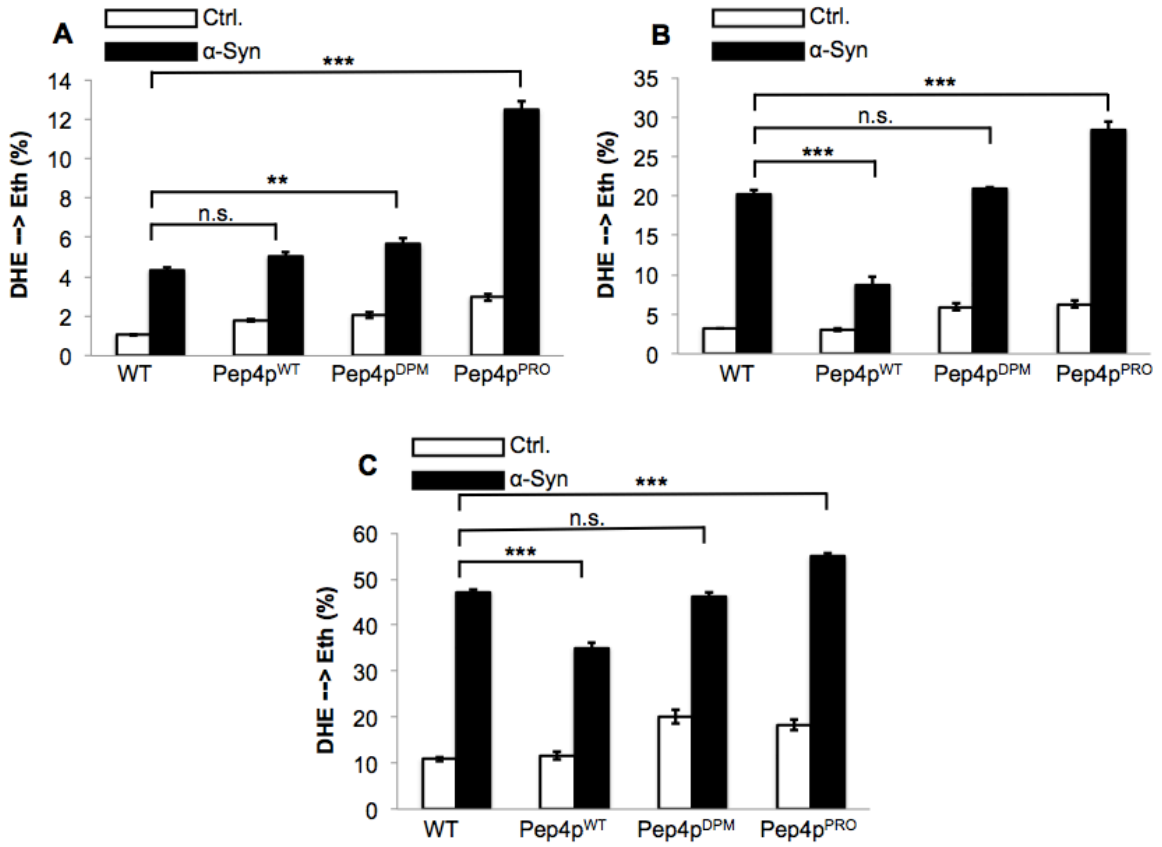

Figure 5: ROS accumulation indicated by flow cytometric quantification of DHE to Eth conversion of wild type cells (WT), Pep4p wild type (Pep4p^{WT}), double point mutation of Pep4p (Pep4p^{DPM}) and propeptide of Pep4p (Pep4p^{PRO}) expressing cells, with and without co-expression of human α-synuclein (α-Syn). ROS accumulation was analysed 16 h (A), 24 h (B) and 48 h (C) after induction. Means ± s.e.m., n=12. ***P<0.001; **P<0.01; n.s.P>0.05.

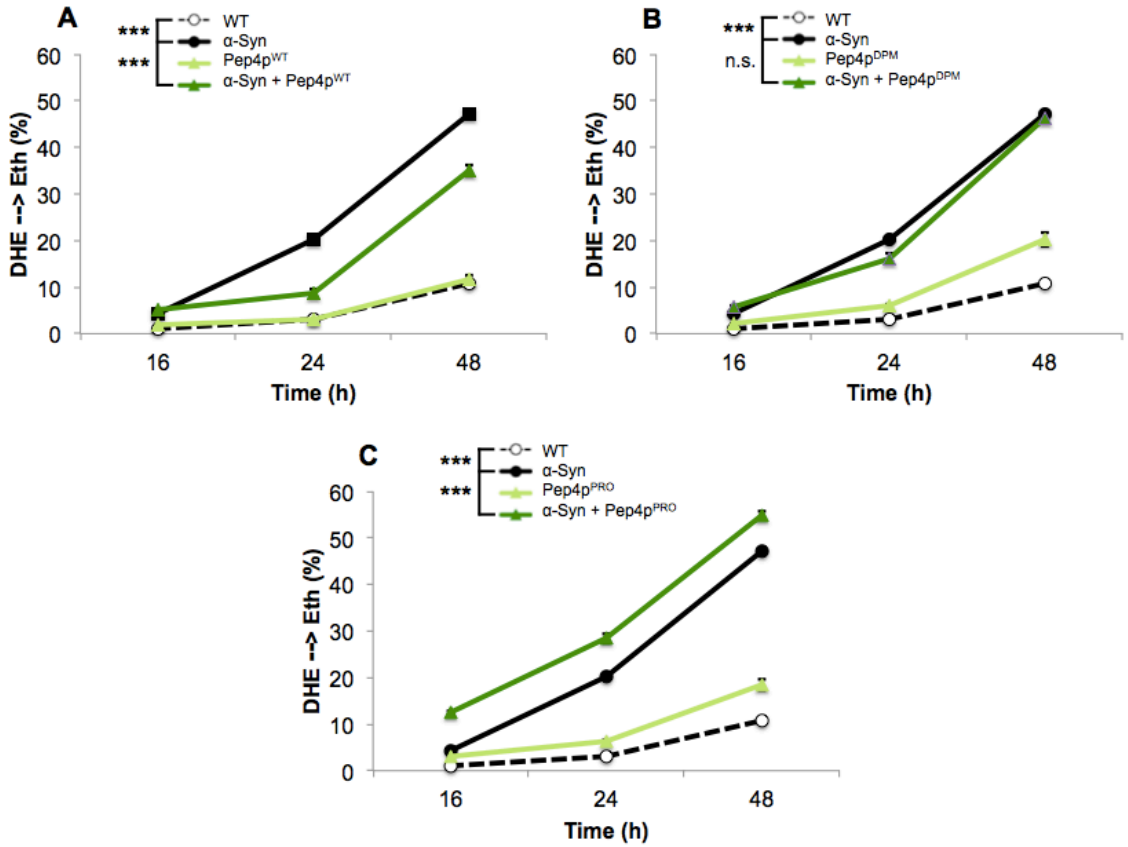

Figure 6: Time course of ROS production indicated by flow cytometric quantification of DHE→Eth conversion of wild type cells (WT), Pep4p wild type (Pep4p^{WT}), double point mutation of Pep4p (Pep4p^{DPM}) and propeptide of Pep4p (Pep4p^{PRO}) expressing cells, with and without co-expression of human α-synuclein (α-Syn). ROS production was analysed 16 h (A), 24 h (B) and 48 h (C) after induction. Means ± s.e.m., n=12. ***P<0.001; n.s.P>0.05.

To detect pre-lethal ROS accumulation, the mean fluorescence signal of DHE negative cells was analysed. This signal was monitored 16 hours after induction and is visualized in Figure 8. The tendency of α-synuclein expressing cells to cause more pre-lethal ROS was seen, but this effect did not show statistical significance. The overexpression of the different Pep4p forms had also no significant influence on the mean fluorescence signal. This is especially interesting in case of overexpressed propeptide, since increased ROS production and cell death was observed in previous experiments.

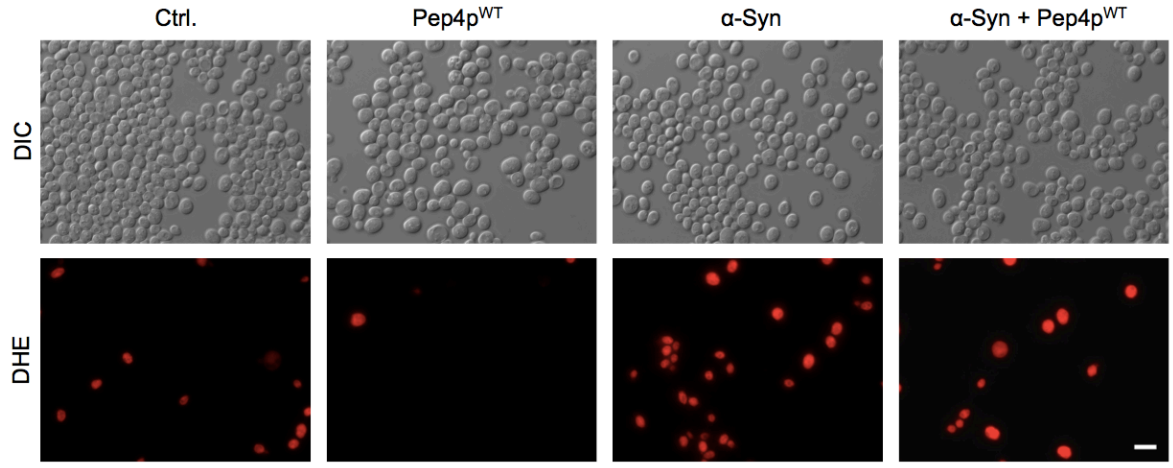

Figure 7: Fluorescence microscopic sample pictures of DHE stained wild type cells (Ctrl.) and Pep4p wild type (Pep4p^{WT}) expressing cells, with and without co-expression of human α-synuclein (α-Syn). After flow cytometric quantification of DHE to Eth conversion, cells were pooled and analysed by fluorescence microscopy to visualize determined ROS accumulation. Scale bar represents 10 µm.

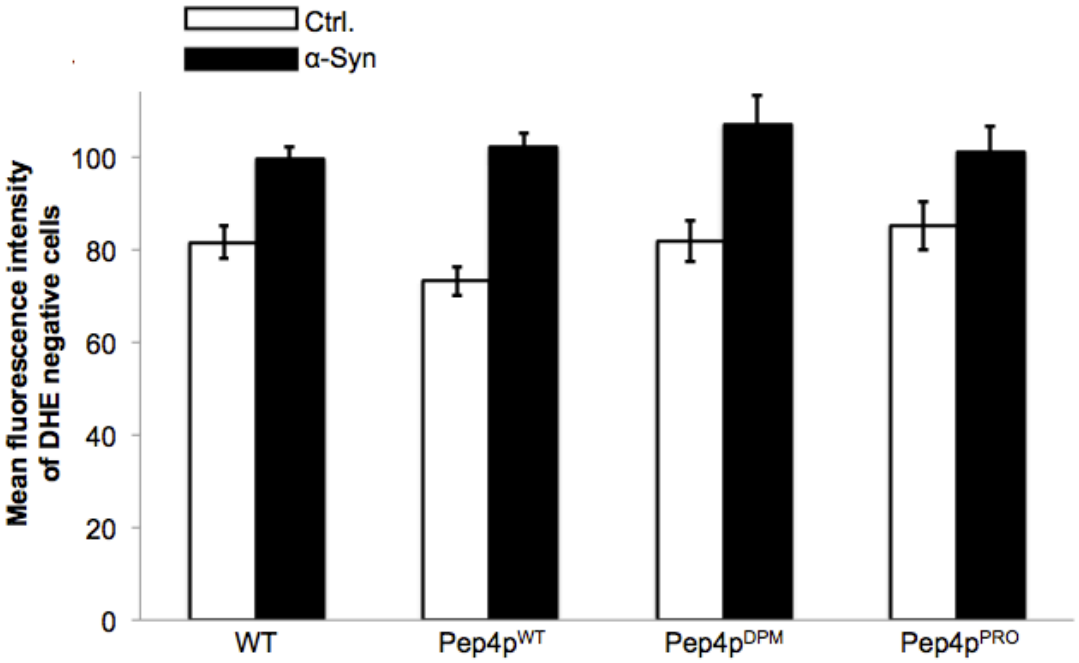

Figure 8:Pre-lethal ROS accumulation indicated by flow cytometric quantification of the mean fluorescence intensity of DHE → Eth negative cells of wild type cells (WT), Pep4p wild type (Pep4p^{WT}), double point mutation of Pep4p (Pep4p^{DPM}) and propeptide of Pep4p (Pep4p^{PRO}) expressing cells, with and without co-expression of human α-synuclein (α-Syn). Means ± s.e.m., n=12.

An important advantage of yeast as a model for cell death is the possibility to determine cell viability very easy by plating a fixed number of cells on agar plates and then quantifying the number of colonies formed. In Figure 9, preliminary data is shown for such an experiment, which was only carried out once. A significant decrease of survival was detected in cells expressing α-synuclein, when plated on plates containing glycerol as carbon source. $Pep4p^{WT}$ co-expression was sufficient to increase cell viability, which indicates that $Pep4p^{WT}$ overexpression was even able to restore α-synuclein-caused defects under aerobe conditions. This is a further hint for reduction of α-synuclein caused ROS by $Pep4p^{WT}$.

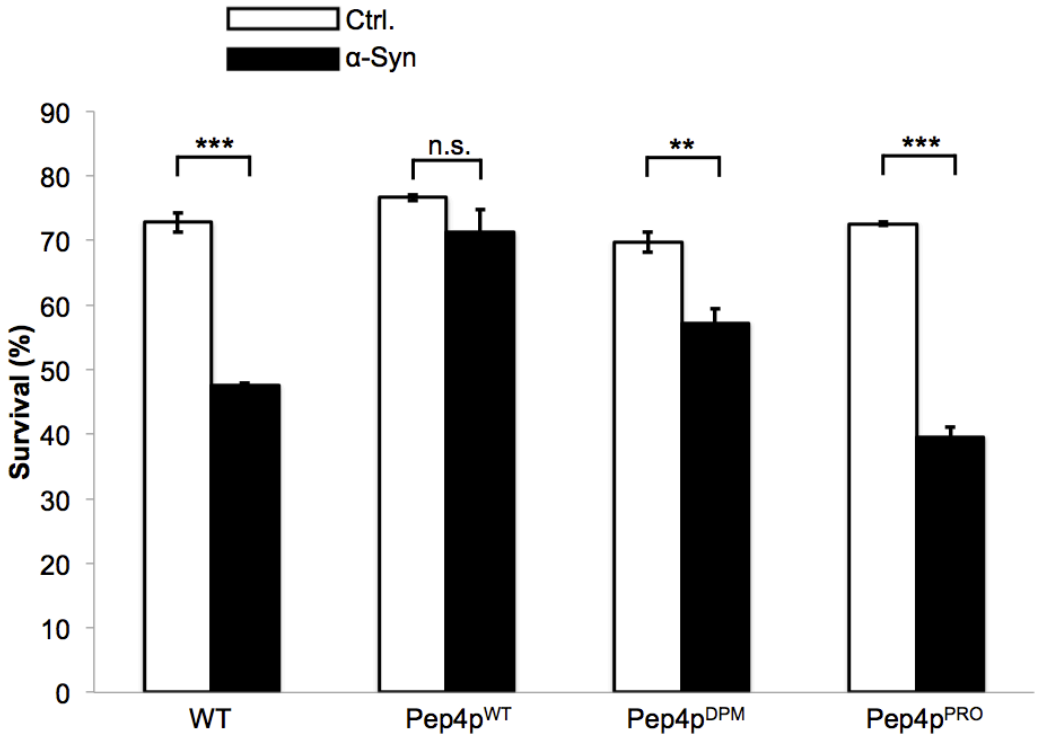

Figure 9: Survival determined by clonogenicity of wild type cells (WT), Pep4p wild type ($Pep4p^{WT}$), double point mutation of Pep4p ($Pep4p^{DPM}$) and propeptide of Pep4p ($Pep4p^{PRO}$) expressing cells, with and without co-expression of human α-synuclein (α-Syn). Cells were plated on YPGly agar plates. 48 hours after induction. Means ± s.e.m., n=3; ***P<0.001; n.s.P>0.05.

To examine the expression in all used clones, immunoblots were performed 24 hours after induction. Therefore, antibodies against the FLAG-epitope were applied to detect Pep4p^{WT}, Pep4p^{DPM}, Pep4p^{PRO} and α-synuclein. Antibodies against glyceraldehyde 3-phosphate dehydrogenase (GAPDH) were used as loading control. Since the propeptide of Pep4p^{WT} has a quite low molecular weight of approximately 10 kDa, a separate gel with 15% polyacrylamide was used for PAGE instead of 12.5% for all other constructs. A sample of this expression control immunoblot is shown in Figure 10. For all other experiments, expression was confirmed this way, but is not explicitly shown in this work.

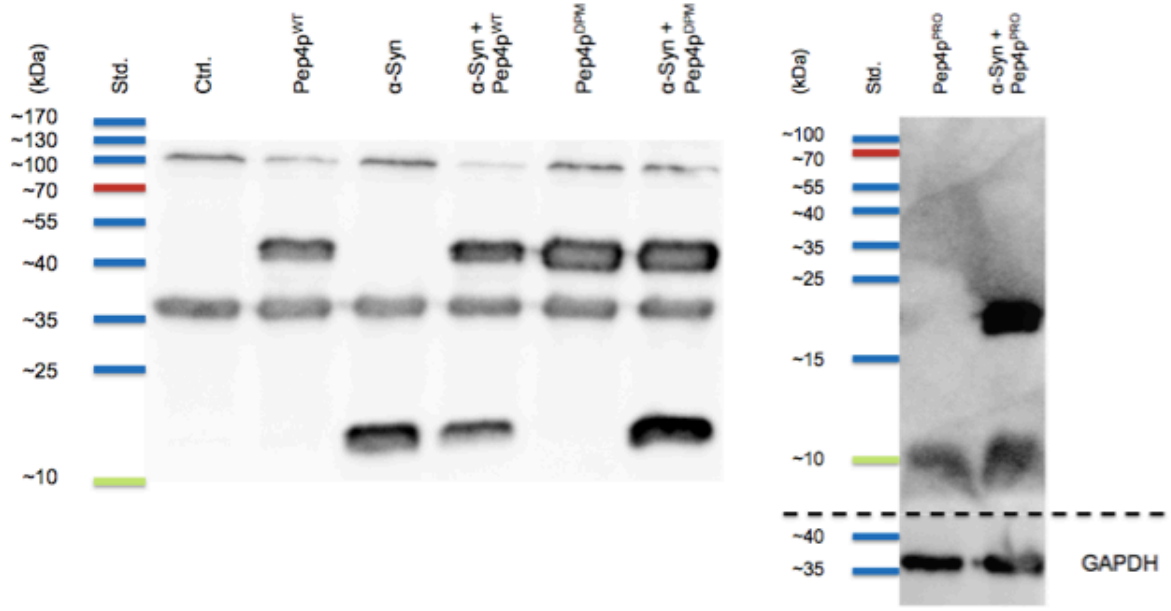

Figure 10: Immunoblot analysis of α-Syn, Pep4p wild type (Pep4p^{WT}), double point mutation of Pep4p (Pep4p^{DPM}) and propeptide of Pep4p (Pep4p^{PRO}) expression using antibodies directed against FLAG epitope and against GAPDH as a loading control.

3.3. α-synuclein caused cytoplasmatic acidification which was prevented by Pep4p

The formation of proteinaceous deposits is a common event in the pathogenesis of many neurodegenerative diseases. In the last few years, evidence emerged that suggests imbalances in pH homeostasis to be a trigger for these toxic events. In Morbus Alzheimer for example, lysosomal acidification deficits lead to a block of autophagy and to the formation of neurotoxic protein aggregates [56]. It was also shown that cytoplasmatic acidification is an event, which occurs during necrotic cell death in neurons [57]. Notably, α-synuclein aggregation was shown to be reinforced at lower pH values [11].

These circumstances led to the question, if α-synuclein causes changes in the pH value of the cytoplasm, and if so, whether the overexpression of $Pep4p^{WT}$ was capable to restore pH homeostasis, since it also decreased cell death. Therefore we used Quinacrine staining as a fast, simple and reproducible method. Quinacrine stained cells were analysed by fluorescence microscopy, as can be seen in Figure 11. Cells containing only the empty vector control, as well as cells only overexpressing $Pep4p^{WT}$ presented a strictly delimited fluorescence signal coming from the vacuole. This indicated low pH values of the vacuole, but not of the cytosol. However, remarkable strong fluorescence signal came from the cytosol in cells expressing only α-synuclein. In most cells of this expression type, the vacuole could not be clearly distinguished from the cytoplasm, since the whole cells showed a positive Quinacrine staining. These results suggested a cytoplasmatic acidification caused by α-synuclein. In fact, most cells co-expressing α-synuclein and $Pep4p^{WT}$ presented again a fluorescence signal only coming from the vacuoles. This indicates that the overexpression of $Pep4p^{WT}$ relieved cytoplasmatic acidification caused by α-synuclein.

Quinacrine staining was also performed with cells overexpressing Pep4p^{DPM} and Pep4p^{PRO}. No alleviation of α-synuclein-caused cytoplasmatic acidification could be observed in these cells. Microscopic sample pictures of Quinacrine stained Pep4p^{DPM} and Pep4p^{PRO} expressing cells are shown in supplementary figure S 2.

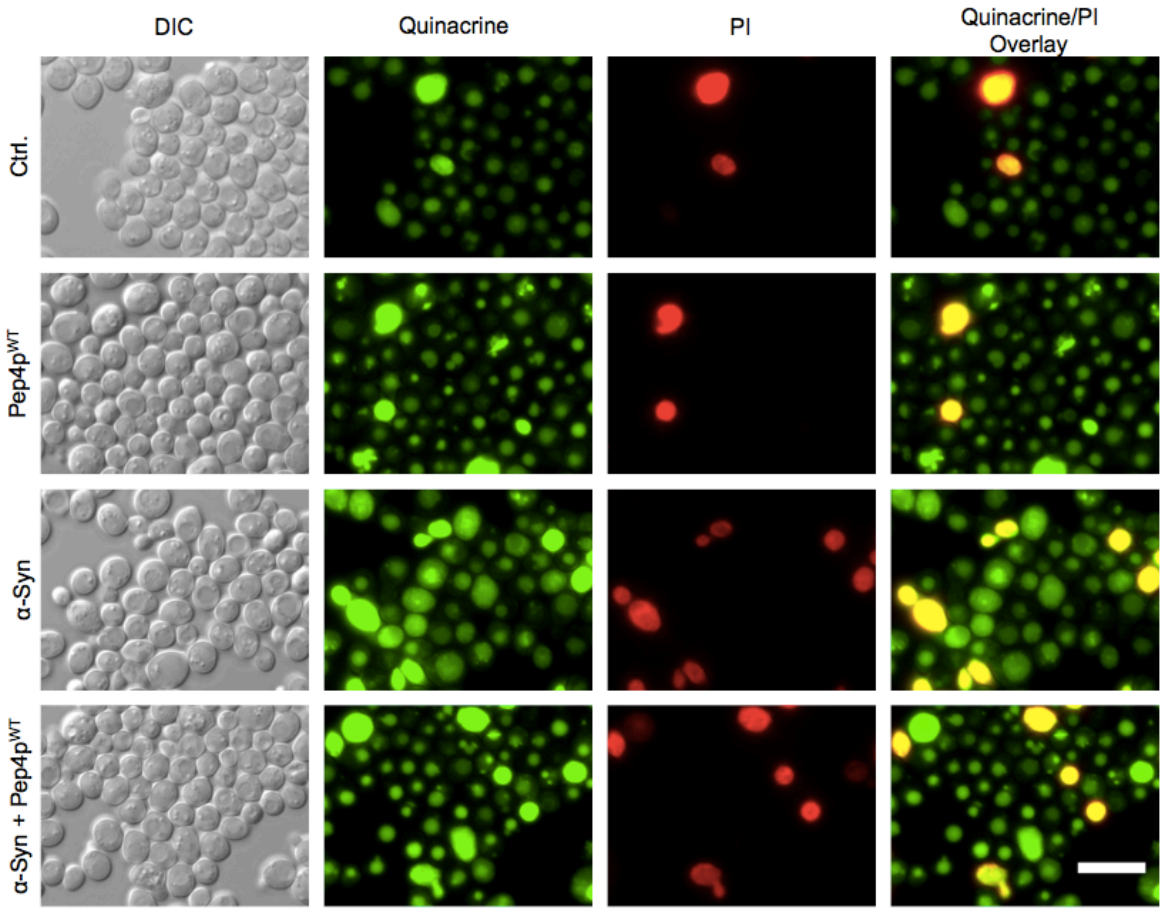

Figure 11: Fluorescence microscopic sample pictures of Quinacrine stained wild type cells (Ctrl.) and Pep4p wild type (Pep4p^{WT}) expressing cells, with and without co-expression of human α-synuclein (α-Syn) 24 hours after induction. Quinacrine staining was used to indicate acidic parts of the cells. Scale bar represents 10 µm.

To quantify the effects on cytoplasmatic acidification, cells with an acidic cytosol were manually counted. For this purpose, at least 450 viable cells (PI positive cells were excluded) per clone were evaluated, and three different clones per expression type were averaged. The percentage of cells with an acidic cytoplasm is presented in Figure 12. This representation shows a significant cytosolic acidification caused by α-synuclein and a significant reduction of this effect by co-expression of Pep4p^{WT}. Pep4p^{DPM} and Pep4p^{PRO} overexpression were not able to restore pH homeostasis.

It conclusion, cytosolic acidification seemed to be a pre-lethal event in α-synuclein cytotoxicity, and the cytoprotective action of Pep4p^{WT} was likely to work through an alleviation of cytoplasmatic acidification.

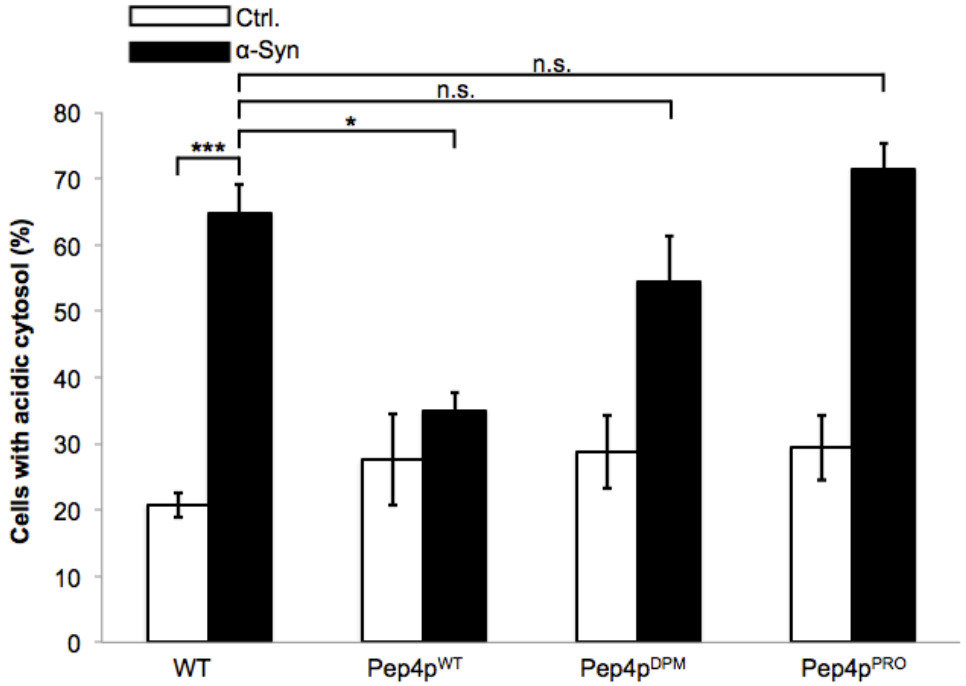

Figure 12: Quantification of cells with acidic cytosol indicated by Quinacrine staining of wild type (WT), Pep4p wild type (Pep4p^{WT}), double point mutation of Pep4p (Pep4p^{DPM}) and propeptide of Pep4p (Pep4p^{PRO}) expressing cells, with and without co-expression of human α-synuclein (α-Syn). Means ± s.e.m., n=3. ***P<0.001; *P<0.05; n.s.P>0.05

3.4. α-synuclein impaired vacuolar morphology

By staining cells with Quinacrine, it was observed that some of the cells only expressing Pep4p^{WT} showed quite a high number of vacuoles, compared to the empty vector control. To investigate changes in the vacuolar morphology, microscopic analysis of MDY-64 staining was performed, which selectively stains the vacuolar membrane.

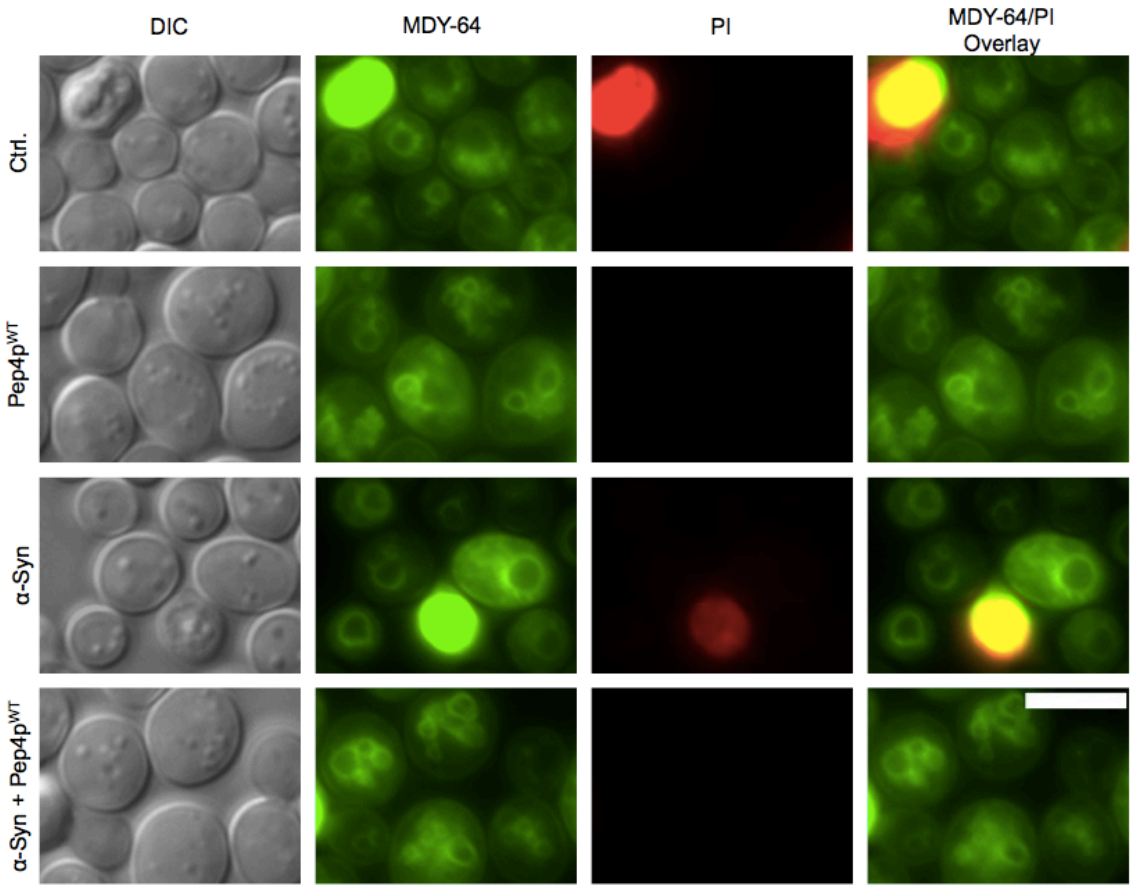

Figure 13: Fluorescence microscopic sample pictures of MDY-64 stained wild type cells (Ctrl.) and Pep4p wild type (Pep4p^{WT}) expressing cells, with and without co-expression of human α-synuclein (α-Syn) 16 hours after induction. MDY-64 staining was used to display vacuolar morphology. Scale bar represents 5 µm.

Representative pictures of the MDY-64 staining, performed 16 hours after induction, are shown in Figure 13. Cells carrying the empty vector control appeared with a mixture of vacuolar morphologies, containing low and high numbers of vacuoles. Pep4p^{WT} overexpression led to a shift of this ratio to a high number of cells containing more than 6 quite small vacuoles. This observation confirmed the assumed morphology from Quinacrine staining. Interestingly, α-synuclein also led to a change in the vacuolar morphology, but instead of producing this high vacuolar number, α-synuclein had the opposite effect.

Most cells expressing α-synuclein had a lower number of vacuoles, which is normally known from cells in later stages of aging. The co-expression of Pep4p^{WT} somehow seemed to restore the vacuolar phenotype, similar to wild type cells. To quantify this effect, the number of vacuoles per cell was counted in at least 400 viable cells (PI positive cells were excluded) per clone, whereby three different clones per expression type were averaged. Therefore cells were divided into two groups: three or less vacuoles per cell and more than three vacuoles per cell. This quantification is presented in Figure 14. The percentage of cells with three or less vacuoles was massively increased in cells expressing α-synuclein. The opposite effect was observed in cells only expressing Pep4p^{WT}, which significantly reduced the number of cells with three or less vacuoles. The co-expression led to a restoration of the vacuolar morphology with no significant differences compared to the empty vector control.

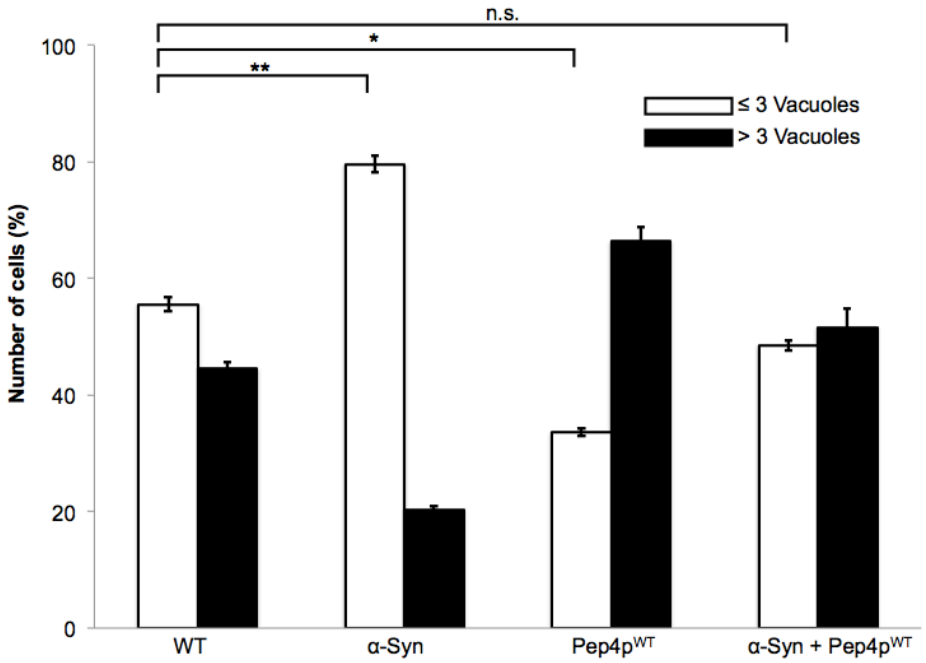

Figure 14: Quantification of vacuoles per cell indicated by MDY-64 staining of wild type (WT) and Pep4p wild type (Pep4p^{WT}) expressing cells, with and without co-expression of human α-synuclein 16 hours after induction. Means ± s.e.m., n=3. **P<0.01; *P<0.05; n.s.P>0.05

The same experiment was done 24 hours after induction of expression (Figure 15). As a normal process of vacuolar maturation, cells of the empty vector control displayed a reduced number of vacuoles per cell, so that no difference between the vacuolar phenotype of control cells and α-synuclein expressing cells could be observed. The vacuolar phenotype produced by Pep4p^{WT} overexpression however, was still seen 24 hours after induction.

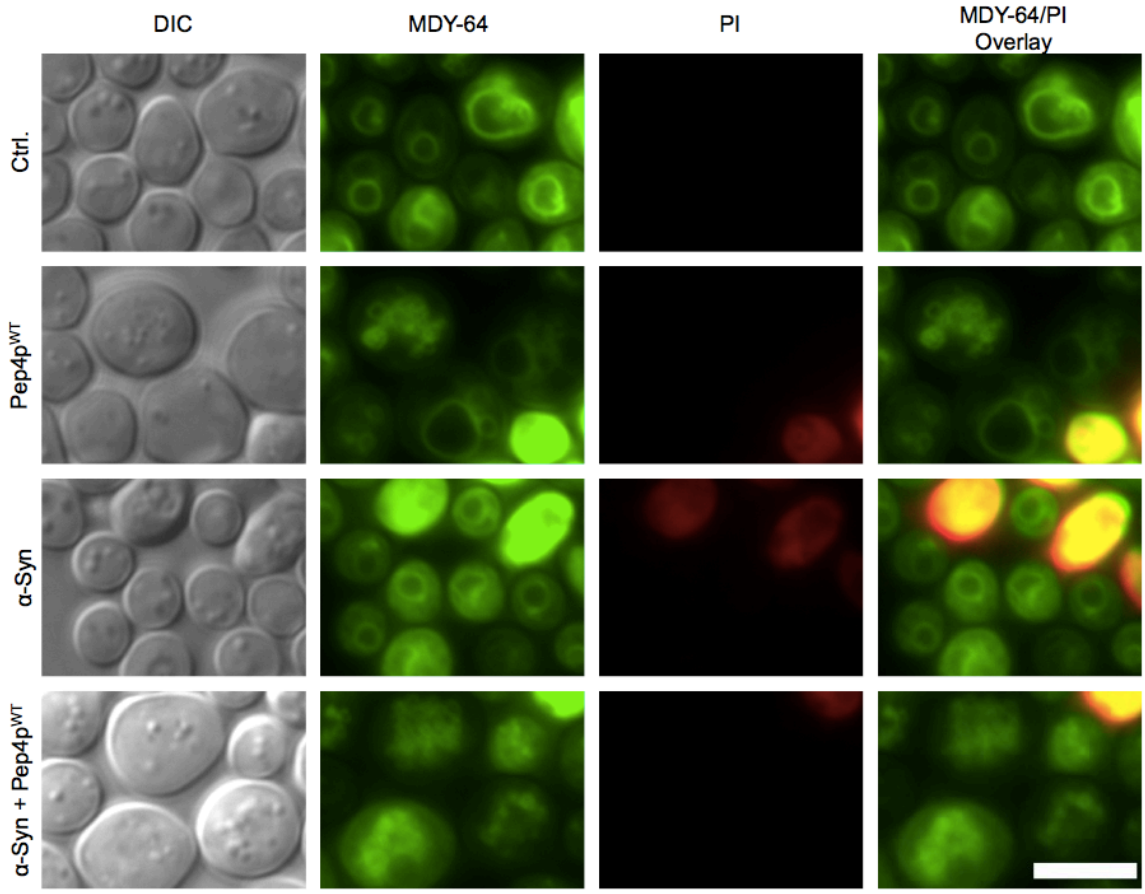

Figure 15: Fluorescence microscopic sample pictures of MDY-64 stained wild type cells (Ctrl.) and Pep4p wild type (Pep4p^{WT}) expressing cells, with and without co-expression of human α-synuclein (α-Syn) 24 hours after induction. MDY-64 staining was used to display vacuolar morphology. Scale bar represents 5 µm.

Quantification of these pictures demonstrated no significant differences between the empty vector control and α-synuclein expressing cells after 24 hours (Figure 16). But the vacuolar morphology caused by Pep4p^{WT} still showed this high number of small vacuoles. The group of 3 or less vacuoles per cell was significantly smaller in Pep4p^{WT} cells compared to the empty vector control. And again, the co-expression of α-synuclein led to a higher number of cells in the group with 3 or less vacuoles compared to Pep4p^{WT} cells, yet the number of cells in this group was significantly lower than compared to control or α-synuclein expressing cells.

Since Pep4p^{WT} expression reduced cell death caused by α-synuclein, it is likely that the vacuolar morphology caused by Pep4p^{WT} contributes to this survival benefit.

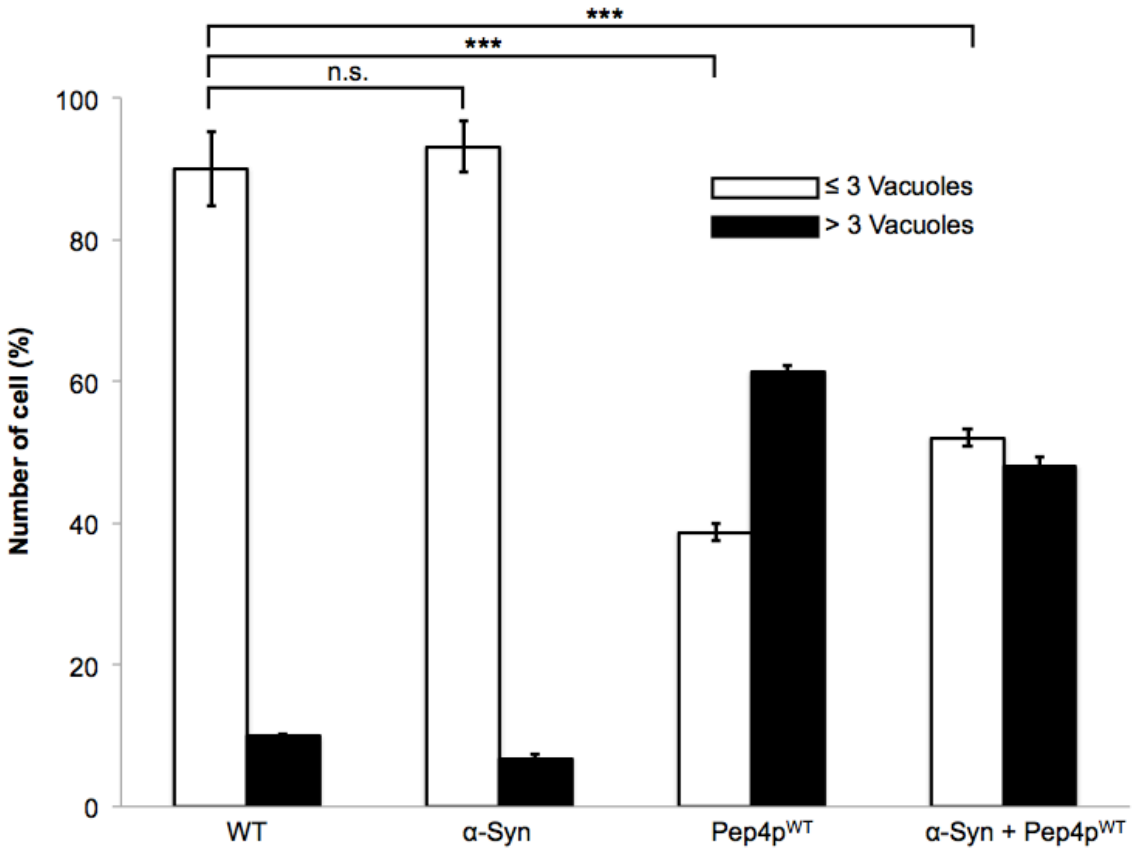

Figure 16: Quantification of vacuoles per cell indicated by MDY-64 staining of wild type (WT) and Pep4p wild type (Pep4p^{WT}) expressing cells, with and without co-expression of human α-synuclein 24 hours after induction. Means ± s.e.m., n=3. ***P<0.001; n.s.P>0.05

3.5. α-synuclein did not cause vacuolar membrane permeabilization

Because previous experiments showed cytosolic acidification, increased cell death and changes of vacuolar morphology in α-synuclein expressing cells, a rupture of the vacuolar membrane caused by α-synuclein could be involved. This process is known as lysosomal membrane permeabilization (LMP) in mammalian cells and causes cell death [58]. The hypothesis underlying this experiment was, that observed changes of the vacuolar membrane caused by α-synuclein also cause LMP, which might lead to the cytoplasmatic acidification displayed in Quinacrine staining experiments.

To investigate LMP, here referred as vacuolar membrane permeabilization (VMP), since experiments were carried out in yeast, FITC-coupled dextrans with molecular weights reaching from 10 kDa to 250 kDa were used. These dextrans are known to be taken up via endocytosis and are then transported into the vacuoles [59]. If VMP occurs, the localization of the fluorescence signal would be seen in the cytoplasm.

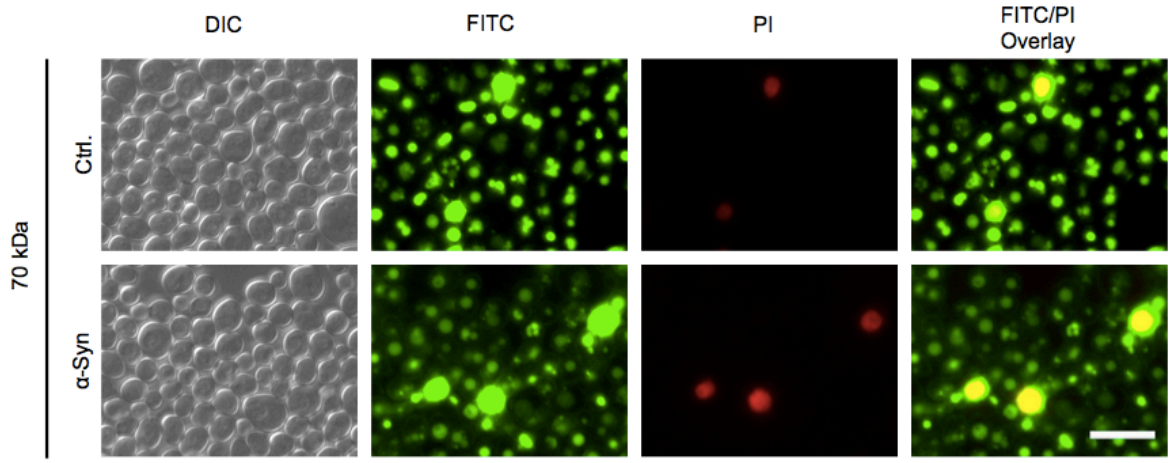

Figure 17: Fluorescence microscopic sample pictures of wild type cells (Ctrl.) with and without co-expression of human α-synuclein (α-Syn) incubated with FITC-coupled dextrans (70 kDa) to detect vacuolar membrane permeabilization (VMP). Scale bar represents 10 µm.

Cells expressing α-synuclein were compared to the empty vector control 16 hours after induction. Figure 17 displays results from fluorescence microscopy, using FITC-coupled dextrans with an average molecular weight of 70 kDa. It can be seen in this pictures that the only detectable fluorescence signal came from the vacuole. Fluorescence microscopic pictures of FITC-coupled dextrans with molecular weights of 10, 40 and 250 kDa are presented in the supplementary figure S 3. Even with smaller molecular weights than 70 kDa, no VMP could be observed. Therefore it is likely, that α-synuclein did not cause VMP.

3.6. Pep4p overexpression reduced α-synuclein oligomers

Lewy bodies, the hallmark of PD, mainly consist of α-synuclein and seem to be formed via its aggregation [3, 60]. Since it was observed in mouse models that moderate overexpression of α-synuclein led to its aggregation in presynaptic terminals [61] the question was raised, if the observed reduction of cell death through $Pep4p^{WT}$ is caused by degradation of toxic α-synuclein aggregates. As available literature indicates that oligomeric forms of α-synuclein are more toxic than fibrils [62], these species were of special interest.

In order to detect α-synuclein oligomers, a semi-native immunoblot was performed with an α-synuclein-specific antibody. This semi-native approach has the advantage of producing sharper bands than a blue native immunoblot, which was crucial in this experiment, because of the quite small differences in the molecular weights of the resulting bands.

Figure 18 shows a sample of the performed semi-native immunoblots. In addition to the monomeric α-synuclein band with about 17 kDa, specific α-synuclein bands appeared with a molecular weight of about 30, 35, 38 and 40 kDa. It can be clearly seen that the co-expression of $Pep4p^{WT}$ led to a reduced intensity of all α-synuclein bands in these immunoblots. Using GAPDH as a loading control allowed quantification of the relative intensities. Figure 18 shows that with the exception of monomeric band, all observed α-synuclein bands were significantly reduced by co-expression of $Pep4p^{WT}$.

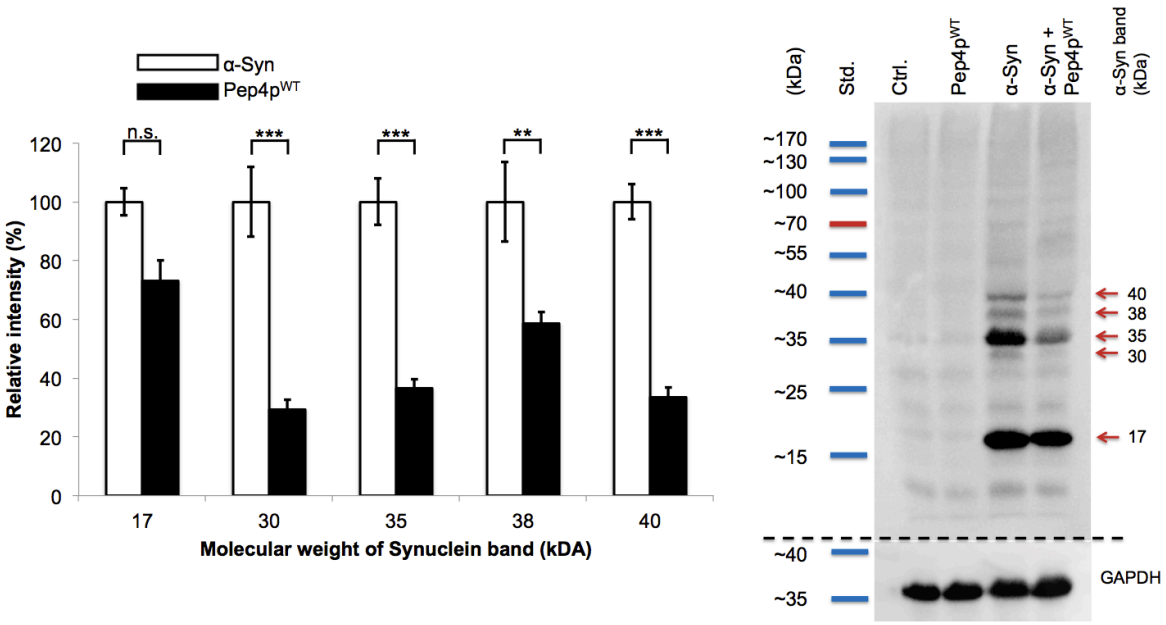

Figure 18: Sample of a semi-native immunoblot and quantification of the relative intensity using an α-synuclein antibody to detect oligomeric forms and GAPDH as loading control. Samples were taken 24 hours after induction. Means ± s.e.m.; n=6. ***P<0.001; n.s.P>0.05

3.7. α-synuclein inhibited vacuolar breakdown in autophagy

Since there is multiple evidence that α-synuclein blocks autophagy [63], it was decided to analyse the effects of α-synuclein expression on autophagy in the yeast model used in this work and with simultaneous co-expression of $Pep4p^{WT}$.

To investigate autophagy, a yeast strain with endogenous GFP-tagged Atg8p was used. Because this protein is localized at autophagosomes, where it is involved in phagophore expansion, its expression and in particular its localization to autophagosomal structures is an indicator for the induction of autophagy. Since it is transported to the vacuole during autophagosomal clearance, it can be also used for monitoring vacuolar breakdown and the efficiency of autophagy. By performing immunoblots with an anti-GFP antibody the induction/repression of autophagy was assessed via the Atg8p-GFP signal. As a hint for the efficiency of autophagy, the free GFP was quantified, which is generated via vacuolar degradation of Atg8p-GFP. Such immunoblots were performed 16 hours (Figure 19 A) and 24 hours (Figure 19 B) after induction. Since this experiment was carried out only once (n=4), only preliminary data are shown.

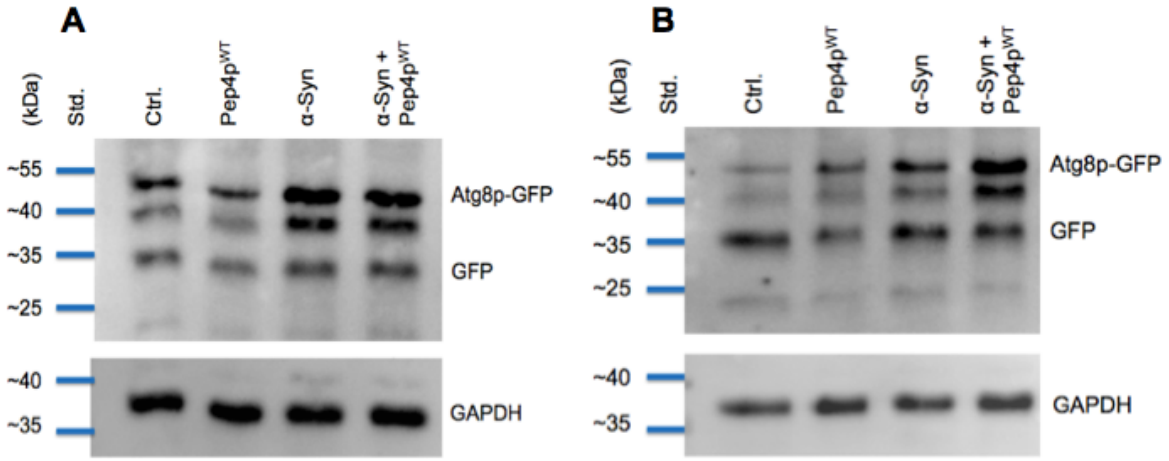

Figure 19: Immunoblot analysis of endogenous GFP-tagged Atg8p in α-synuclein (α-Syn) and Pep4p wild type ($Pep4p^{WT}$) expressing cells, using antibodies directed against GFP and GAPDH as a loading control. Samples were taken 16 hours (A) and 24 hours (B) after induction.

The Atg8p-GFP/GAPDH ratio was densitometrically quantified (Figure 20) to evaluate the impact of α-synuclein and of Pep4p^{WT} on the expression levels of Atg8p. This ratio suggested a significant induction of Atg8p expression caused by α-synuclein as early as 16 hours after expression started. After 24 hours a further up-regulation of Atg8p expression in α-synuclein expressing cells was seen by co-expression of Pep4p^{WT}. However, this effect was not statistically significant in this small-sized determination.

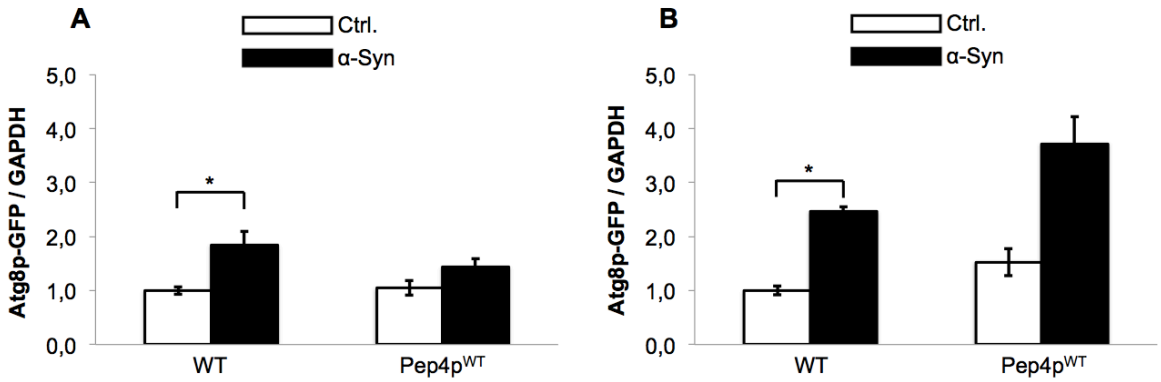

Figure 20: Quantification of the Atg8p-GFP/GAPDH ratio as an indicator of autophagy. Immunoblots of endogenous GFP-tagged Atg8p expressing cells were analysed 16 hours (A) and 24 hours (B) after induction. Means ± s.e.m.; n=4. *P<0.05

Next, the ratio of free GFP/Atg8p-GFP was determined as a mean to quantify the efficiency of autophagy (Figure 21). After 16 hours a reduction of this ratio was observed, which further decreased 24 hours after induction. This indicated a significant impact of α-synuclein on autophagic flux. A slight increase of the free GFP/Atg8p-GFP ratio was observed by Pep4p^{WT} expression, which severely declined 24 hours after induction. Thus, the autophagic flux is blocked by α-synuclein, and high levels of Pep4p^{WT} are not sufficient to re-install autophagy. However, it should be considered, that Pep4p^{WT} overexpression might lead to such a high vacuolar breakdown that all free GFP was degraded before any signal could be detected.

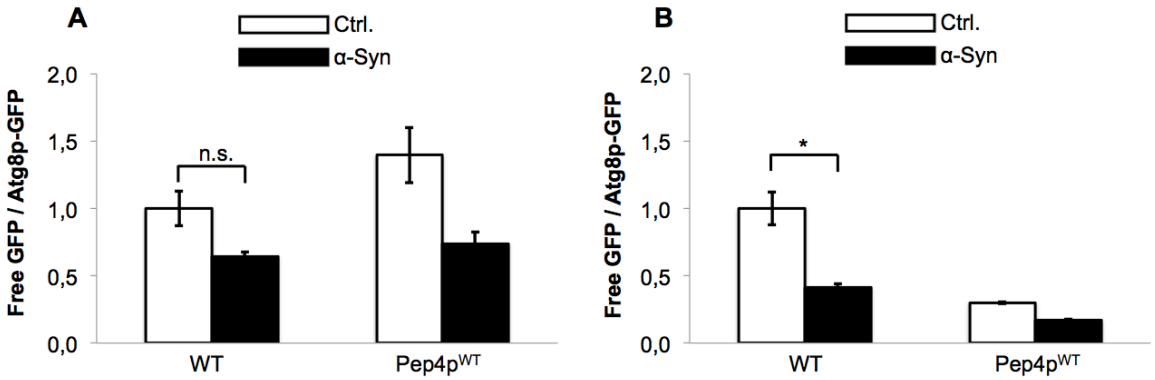

Figure 21: Quantification of the free GFP/Atg8p-GFP ratio as an indicator of autophagy efficiency. Immunoblots of endogenous GFP-tagged Atg8p expressing cells were analysed 16 hours (A) and 24 hours (B) after induction. Means ± s.e.m.; n=4. *P<0.05; n.s.P>0.05

Fluorescence microscopy was used 24 hours after induction of expression to monitor the accumulation of autophagosomes (Figure 22). To exclude dead cells, PI staining was performed. Quantification of these pictures demonstrated a significant increase of visible autophagosomes in α-synuclein expressing cells (Figure 23 A). This quantification was not done for cells expressing $Pep4p^{WT}$, because the vacuolar phenotype induced in these cells did not allow a clear distinction between autophagosomes and vacuoles.

Cells with an appropriate autophagic flux should show a fluorescence signal mainly in the vacuole, but not in the cytosol. A significant reduction of these cells was observed when expressing α-synuclein compared to wild type cells (Figure 23 B). Surprisingly, a lower amount of autophagic cells was also detected in $Pep4p^{WT}$ expressing cells.

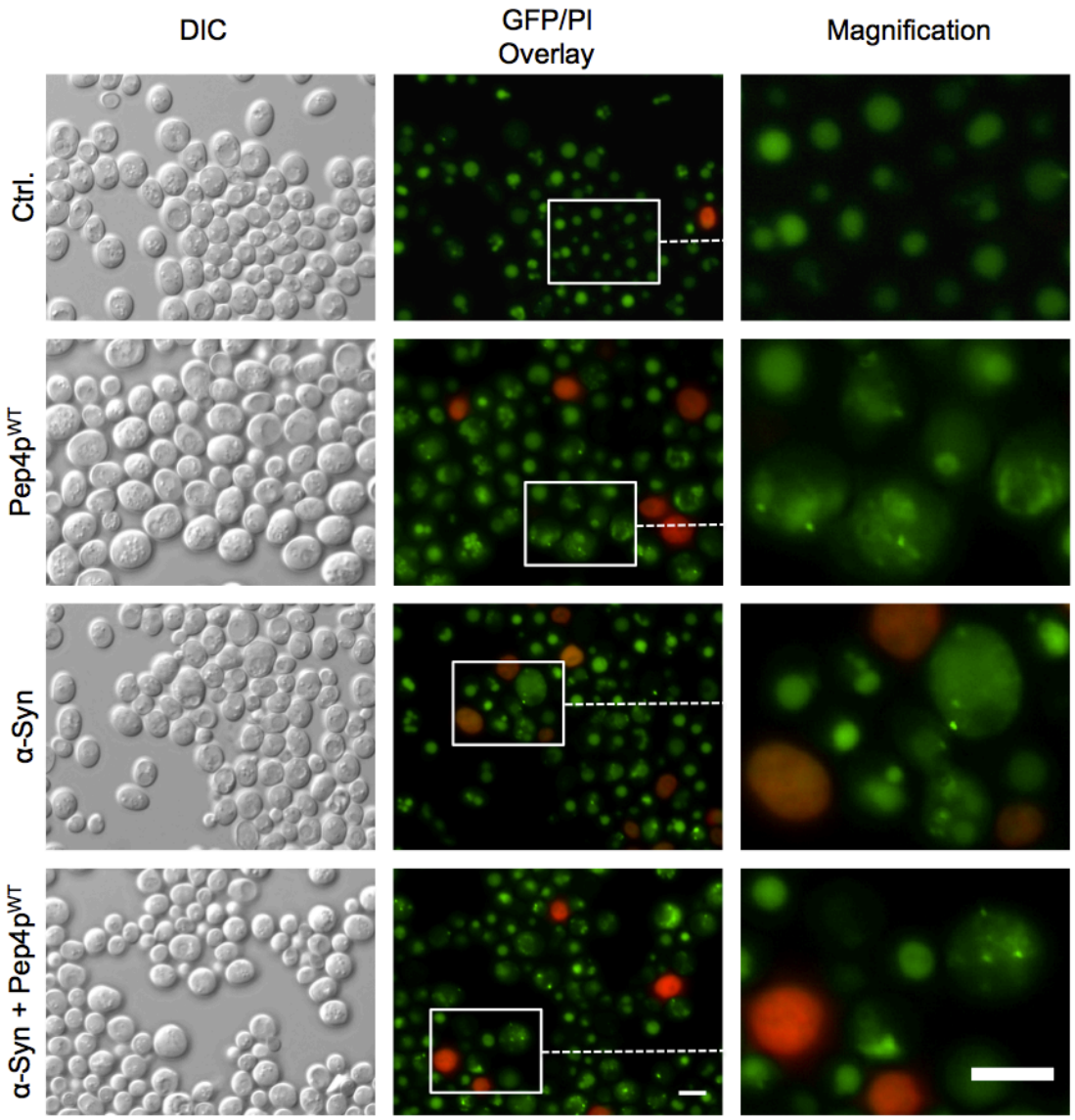

Figure 22: Fluorescence microscopic sample pictures of endogenous GFP-tagged Atg8p expressing cells to monitor autophagy and autophagosome accumulation. Wild type cells (Ctrl.) and Pep4p wild type (Pep4p^{WT}) expressing cells, with and without co-expression of human α-synuclein (α-Syn) were observed 24 hours after induction. Scale bars represent 5 µm.

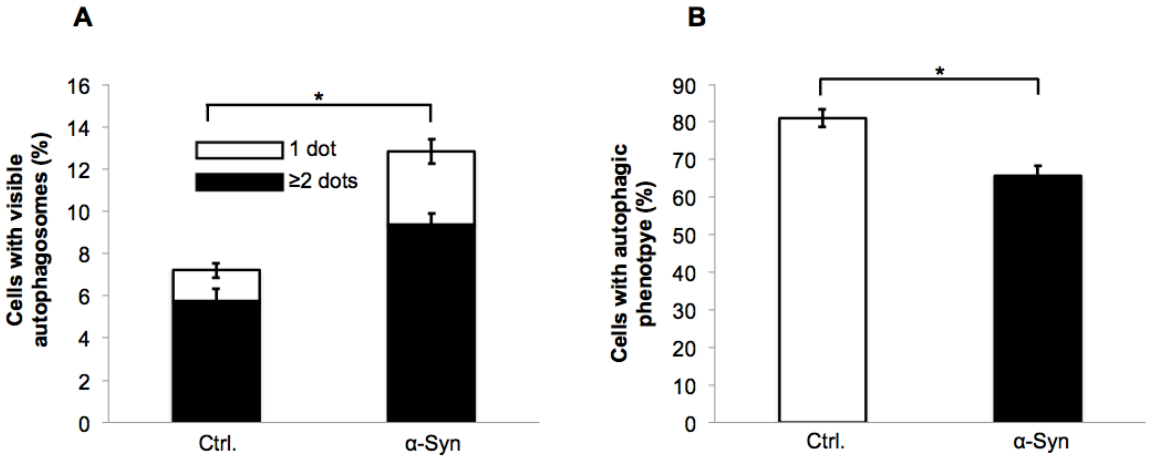

Figure 23: Quantification of autophagosomes (A) and cells with autophagic phenotype (B) in Atg8p-GFP expressing cells 24 hours after induction. Means ± s.e.m.; n=3. *P<0.05

To monitor, if the endogenous GFP-tag of Atg8p has any influence on α-synuclein cytotoxicity and the protective effects of Pep4p^{WT}, PI staining followed by FACS analysis of these cells was performed. As shown in Figure 24, α-synuclein caused an increase of cell death and Pep4p^{WT} overexpression was again sufficient to reduce this effect. Furthermore, the production of ROS was determined by fluorescence microscopy of DHE stained cells (Figure 25). These pictures indicated a higher ROS production caused by α-synuclein, which was alleviated by Pep4p^{WT} co-expression.

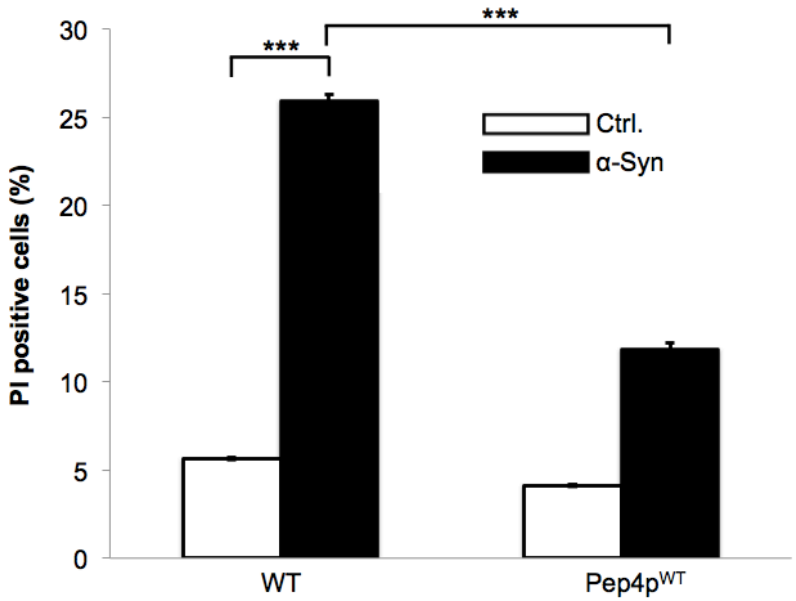

Figure 24: Cell death indicated by flow cytometric quantification of propidium iodide (PI) staining of Atg8p-GFP expressing cells. Wild type (WT) and Pep4p wild type (Pep4p^{WT}) expressing cells were analysed with and without co-expression of human α-synuclein (α-Syn) 24 hours after induction. Means ± s.e.m., n=16. ***P<0.001; *P<0.05; n.s.P>0.05.

In sum, α-synuclein caused an upregulation of Atg8p, accumulation of autophagosomes and a block of autophagic flux and vacuolar breakdown. Results for Pep4p^{WT} co-expression can only be used partially, because of the uncertain reason of the low free GFP signal and the Pep4p^{WT}-induced vacuolar phenotype, which complicated quantification of fluorescence microscopic pictures.

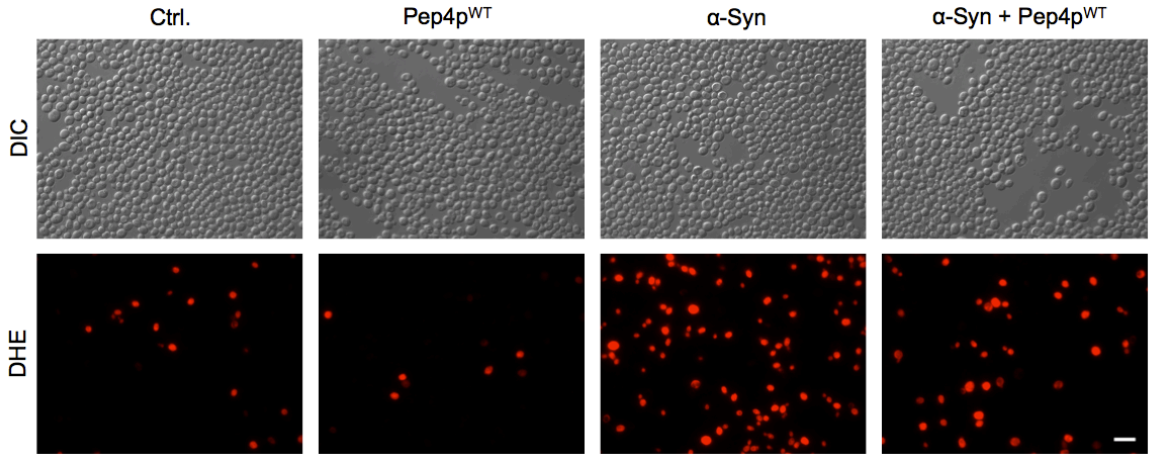

Figure 25: Fluorescence microscopic sample pictures of DHE stained Atg8p-GFP expressing cells. Wild type cells (Ctrl.) and Pep4p wild type (Pep4p^{WT}) expressing cells were analysed with and without co-expression of human α-synuclein (α-Syn) 24 hours after induction. Scale bar represents 10 µm.

3.8. External Ca^{2+} protected from α-synuclein cytotoxicity in a Pep4p dependent manner

As reported earlier [24] α-synuclein caused a raise of cytosolic Ca^{2+} levels. This study identified the Golgi-resident Ca^{2+}/Mn^{2+} ATPase Pmr1p as the mediator of this α-synuclein caused changes. Recent findings of our workgroup also showed that an increased external calcium concentration reduced α-synuclein cytotoxicity (unpublished data), by simply adding Ca^{2+} to yeast cultures in the moment of induction. As shown in this work, α-synuclein blocked autophagy, a process controlled by Ca^{2+} [64]. Since $Pep4p^{WT}$ overexpression also diminished α-synuclein toxicity and proper Ca^{2+} homeostasis is essential for vacuolar function, a potential connection between Pep4p and the protective effect of external Ca^{2+} supplementation was tested.

First it was examined if external addition of Ca^{2+} could further decrease α-synuclein caused cell death in $Pep4p^{WT}$ expressing cells. Therefore, 5 mM of Ca^{2+} were added to yeast cultures in the moment of induction. Since previous work from our laboratory showed the most potent alleviation of α-synuclein toxicity between 24 and 40 hours (unpublished data), cell death was studied via PI staining after 16, 24, 40 and 48 hours. Figure 26 presents the time course of this experiment without adding Ca^{2+} (A) as a control and with the addition of Ca^{2+} in the moment of induction of α-synuclein expression (B). It was shown that the addition of Ca^{2+} led to a decrease of α-synuclein toxicity. The cytoprotective effect of $Pep4p^{WT}$ overexpression was also reproducible in this experiment. The addition of Ca^{2+} to cells expressing $Pep4p^{WT}$ caused a further decline in toxicity (Figure 26 B). For an easier comparison of these effects, cells overexpressing α-synuclein are separately shown with and without the addition of Ca^{2+} in Figure 26 C. As indicated, the overexpression of $Pep4p^{WT}$, as well as the addition of Ca^{2+} significantly reduced α-synuclein-caused cell death. An additive cytoprotective effect of Ca^{2+} and $Pep4p^{WT}$ could be observed especially 40 hours after induction, whereas after 48 hours no additional reduction of PI positive cells was detected.

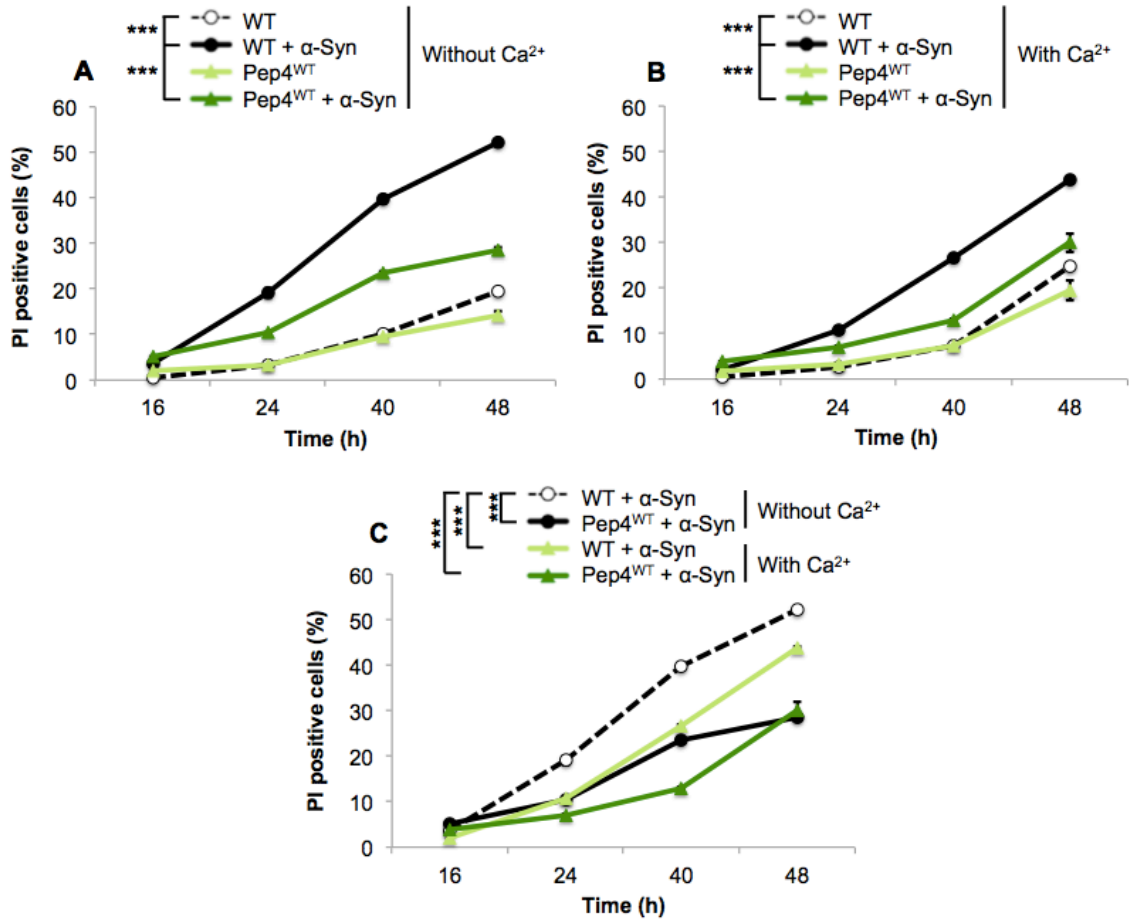

Figure 26: Time course of cell death indicated by flow cytometric quantification of PI stained wild type cells (WT) and Pep4p wild type (Pep4p^{WT}) expressing cells, with and without co-expression of human α-synuclein (α-Syn). Expression was either performed without adding Ca^{2+} (A), or with addition of 5 mM Ca^{2+} in the moment of induction (B). For easier comparison, time course of α-synuclein expressing cells, with and without the addition of Ca^{2+} is separately shown (C). Means ± s.e.m., n=12. ***P<0.001

The same setup was used to analyse ROS production via DHE → Eth conversion. In this experiment, oxidative stress followed the time course of cell death and the same cytoprotective effects of Pep4p^{WT} (Figure 27 A) and Ca^{2+} administration (Figure 26 B) were observed. Additive effects of Pep4p^{WT} and Ca^{2+} were also shown for lowering ROS levels. Figure 27 C separately shows the time course of ROS production for α-synuclein expressing cells, with and without the addition of Ca^{2+}.

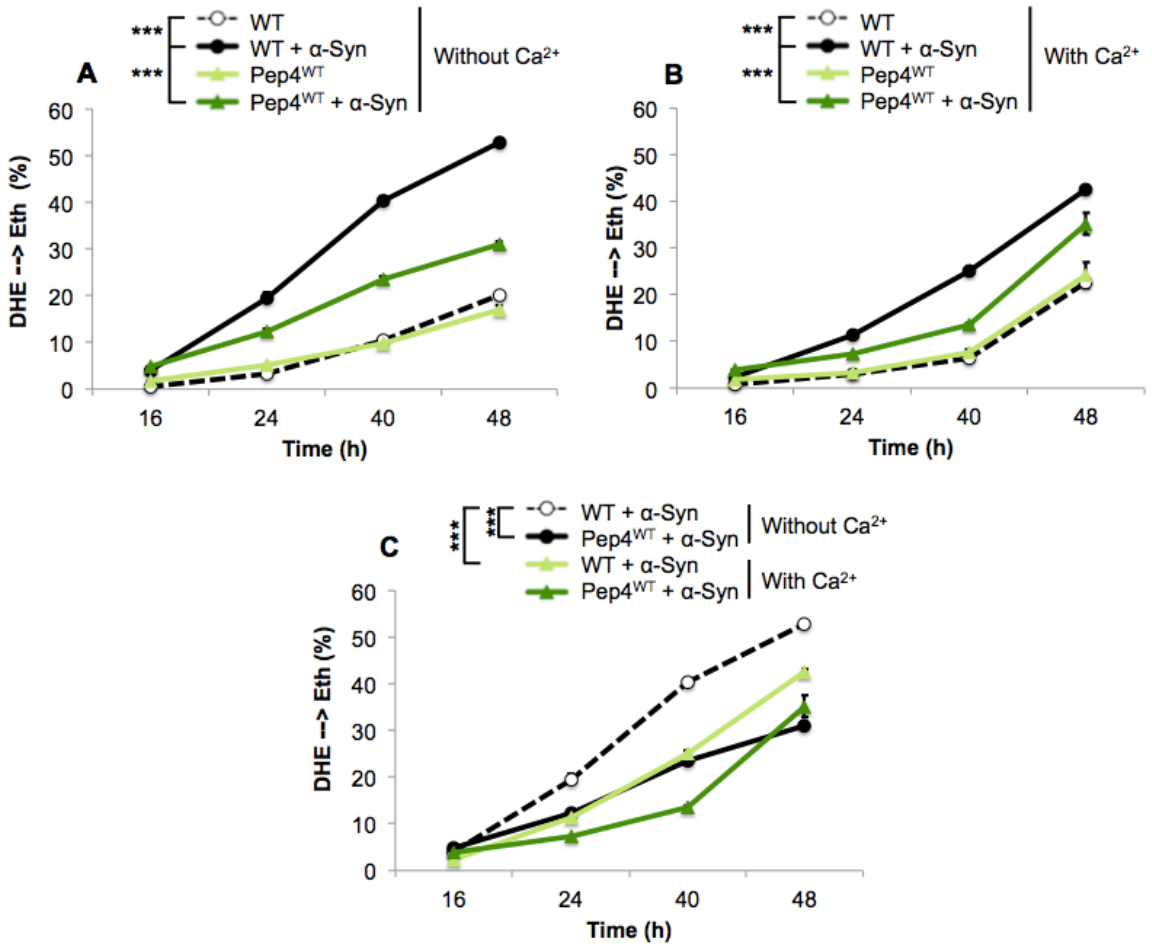

Figure 27: Time course of ROS production indicated by flow cytometric quantification of DHE→Eth conversion of wild type cells (WT) and Pep4p wild type (Pep4p^{WT}) expressing cells, with and without co-expression of human α-synuclein (α-Syn). Expression was either performed without adding Ca^{2+} (A), or with administration of 5 mM Ca^{2+} in the moment of induction (B). For easier comparison, time course of α-synuclein expressing cells, with and without the addition of Ca^{2+} is separately shown (C). Means ± s.e.m., n=12. ***P<0.001

In sum, Pep4p^{WT} and the addition of 5 mM Ca^{2+} had the same cytoprotective effects until 40 hours after induction, but only Pep4p^{WT} still decreased α-synuclein cytotoxicity after 48 hours. An addition of both effects was observed with its most potent cytoprotection 40 hours after induction.

To further investigate a possible role of Pep4p^{WT} in the alleviation of α-synuclein toxicity via Ca^{2+} administration, the same experiment was carried out using a *PEP4* knockout (Δpep4) strain. If Pep4p^{WT} was essentially involved in this Ca^{2+} mediated cytoprotection, the increase of the external Ca^{2+} concentration should not influence cell death or ROS production in absence of Pep4p.

Figure 28 presents this data for cell death indicated via PI staining. In the control experiment without Ca^{2+} (A), Δpep4 cells, at least within the first 48 hours of expression, had no higher level of cell death than wild type cells. The loss of Ca^{2+}-mediated protection against α-synuclein could be very impressively seen when Ca^{2+} was added to Δpep4 cells expressing α-synuclein (B). Cell death was significantly higher in α-synuclein expressing Δpep4 cells when Ca^{2+} was added, than in α-synuclein expressing wild type cells with Ca^{2+} administration. There were no significant differences between α-synuclein expressing wild type cells without Ca^{2+} and α-synuclein expressing Δpep4 cells with Ca^{2+}. As the same time course could be seen in quantification of oxidative stress (Figure 29 A-C), it was concluded that the significant reduction of α-synuclein cytotoxicity by adding 5 mM Ca^{2+} at the moment of induction to yeast cultures required Pep4p.

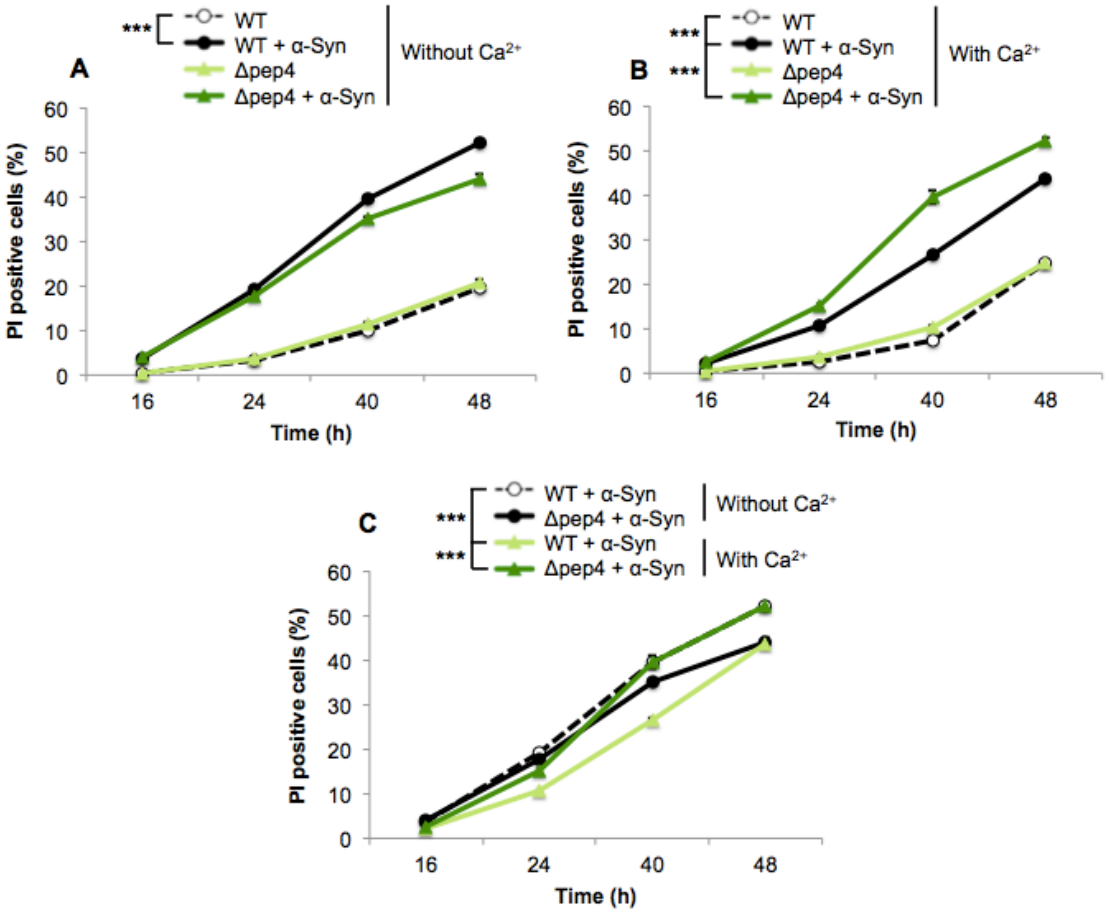

Figure 28: Time course of cell death indicated by flow cytometric quantification of PI stained of wild type cells (WT) and Pep4p knockout (Δpep4) cells with and without expression of human α-synuclein (α-Syn). Expression was either performed without adding Ca^{2+} (A), or with addition of 5 mM Ca^{2+} in the moment of induction (B). For easier comparison, time course of α-synuclein expressing cells, with and without the addition of Ca^{2+} is separately shown (C). Means ± s.e.m., n=12. ***P<0.001

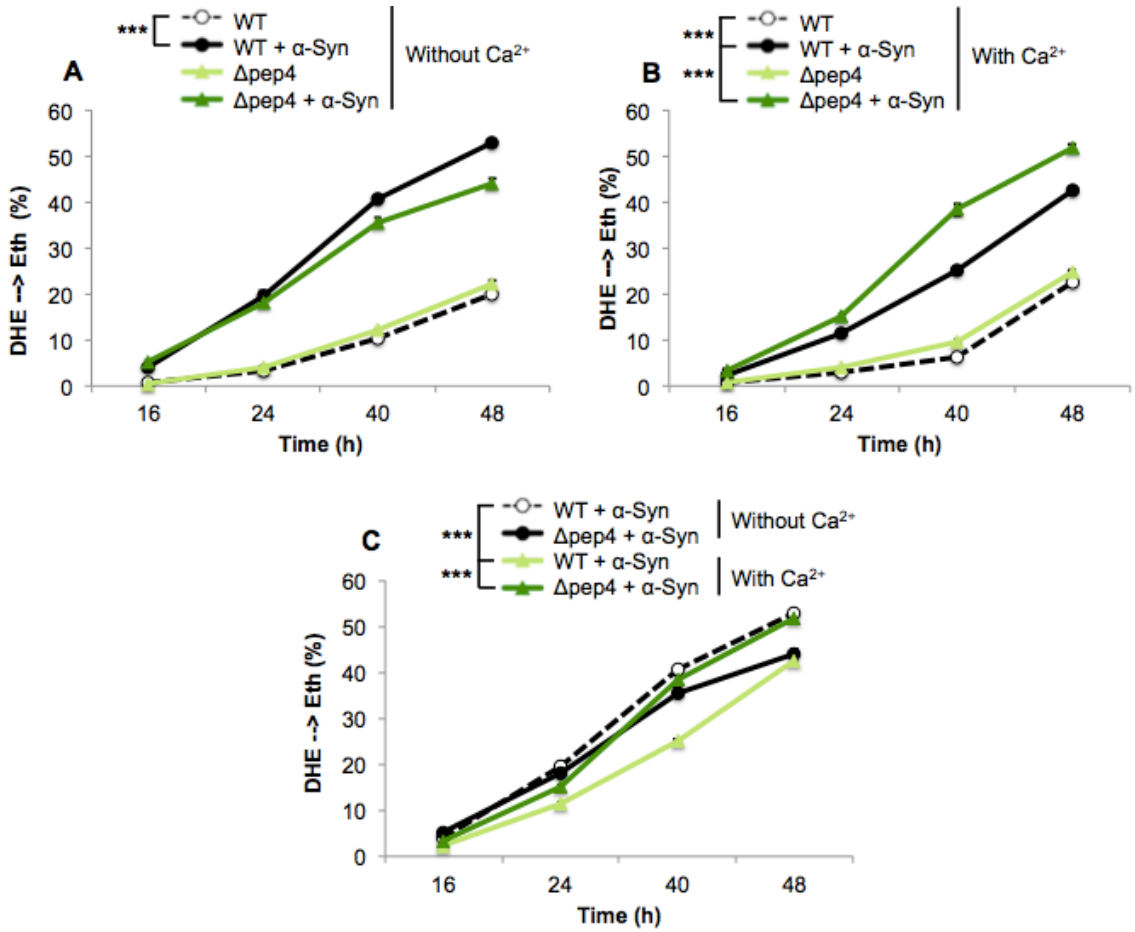

Figure 29: Time course of ROS production indicated by flow cytometric quantification of DHE→Eth conversion of wild type cells (WT) and Pep4p knockout (Δpep4) cells with and without expression of human α-synuclein (α-Syn). Expression was either performed without adding Ca^{2+} (A), or with addition of 5 mM Ca^{2+} in the moment of induction (B). For easier comparison, time course of α-synuclein expressing cells, with and without the addition of Ca^{2+} is separately shown (C). Means ± s.e.m., n=12. ***P<0.001

3.9. α-synuclein reduced enzymatic activity of Pep4p, which was restored by addition of Ca^{2+} in culture

Because overexpression of $Pep4p^{WT}$ declined α-synuclein-caused cytotoxicity, it would be interesting to know, if α-synuclein somehow interfered with endogenously expressed Pep4p. Particularly, a potential change in the localization of Pep4p upon α-synuclein expression and an alteration in the enzymatic activity of Pep4p were analyzed.

To investigate enzymatic activity changes of Pep4p, the empty vector control and α-synuclein expressing cells (both with endogenous Pep4p expression) were examined with a Cathepsin D Activity Assay Kit. 16 hours after induction cells were lysed, and protein concentration was determined with a Bradford assay. For the fluorometric enzyme activity assay, 0.1 µg total cell protein were used. Since previous experiments suggested that Ca^{2+} cytoprotection depends on Pep4p expression, the enzyme activity assay was done with and without the addition of 5 mM Ca^{2+} to yeast cultures in the moment of induction.

A significant reduction of Pep4p activity caused by α-synuclein was observed in cells without Ca^{2+} (Figure 30). When comparing empty vector control cells with and without added Ca^{2+}, a significant increase of Pep4p activity was measured in Ca^{2+} treated cells. As soon as Ca^{2+} was present in the media, a significant higher Pep4p activity could be observed in α-synuclein expressing cells when comparing them to conditions without Ca^{2+}. In presence of Ca^{2+} no significant difference between control cells and α-synuclein expressing cells could be monitored regarding Pep4p activity. This indicated that administration of Ca^{2+} was sufficient to release the block of Pep4p activity caused by α-synuclein, at least in this early phase of expression. Thus, Pep4p activity is reduced by α-synuclein and Ca^{2+} treatment prevented this effect.

The enzymatic activity was also measured in cells overexpressing $Pep4p^{WT}$. In this experiment, higher peptidase activity in these cells was confirmed (see supplementary Figure S 4). Furthermore, a reduction of enzymatic activity in $Pep4p^{WT}$ overexpressing cells caused by α-synuclein was measured but activity in co-expressing cells was still significantly higher than in empty vector control cells.

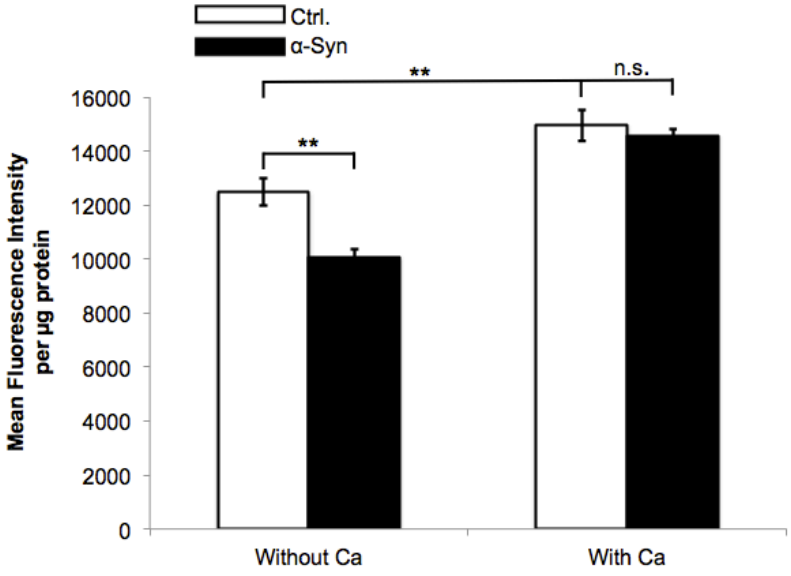

Figure 30: Quantification of Pep4p activity in cells expressing human α-synuclein (α-Syn) 16 hours after induction. Pep4p activity was studied with and without adding 5 mM Ca^{2+} at the moment of induction. Means ± s.e.m., n=8. **P<0.01; n.s.P>0.05

Localization of endogenously GFP-tagged Pep4p ($Pep4p^{GFP}$) was determined with and without heterologous expression of α-synuclein. These cells were analysed by fluorescence microscopy 24 hours after induction, as shown in Figure 31. Pep4p was localized in the vacuole with and without the expression of α-synuclein. Interestingly (and rather unexpectedly), the number of PI positive cells was quite low in cells expressing α-synuclein.

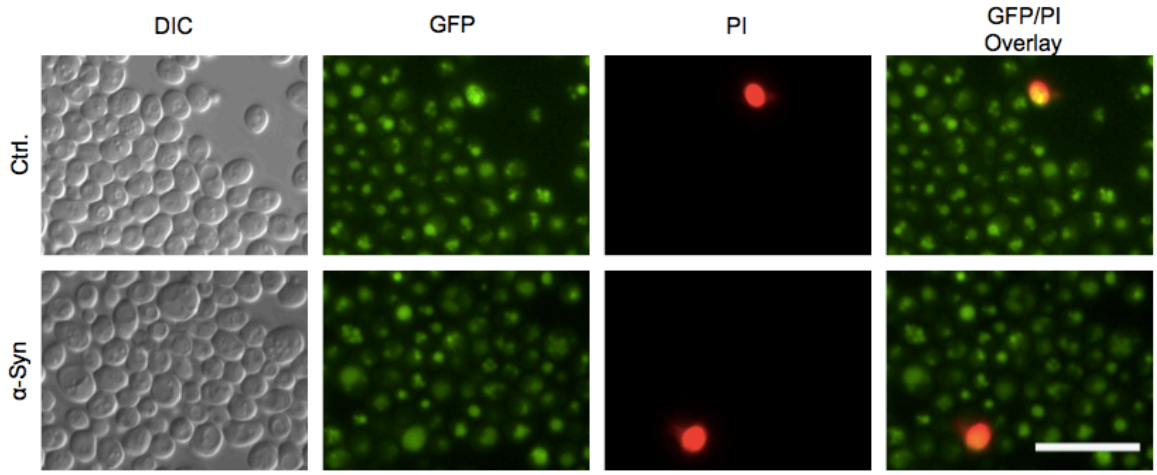

Figure 31: Fluorescence microscopic sample pictures of $Pep4p^{GFP}$ expressing cells with and without co-expression of human α-synuclein (α-Syn). Endogenous GFP-tagged Pep4p was used to analyse localization changes of Pep4p caused by α-synuclein. Since α-synuclein toxicity could not be observed, results were inconclusive. Scale bar represents 10 µm.

Used strains for this experiment were analysed for α-synuclein caused cell death via PI staining and flow cytometric quantification. Indeed, there was no increase in cell death upon α-synuclein expression. Because of the absence of cytotoxicity, the fluorescence microscopy images shown in Figure 31 are inconclusive. Transformation of α-synuclein in Pep4p^{GFP} strains and the above shown experiments were repeated three times without changing the results. α-synuclein expression was also analysed by immunoblotting (Figure 33) to exclude potential differences in expression levels.

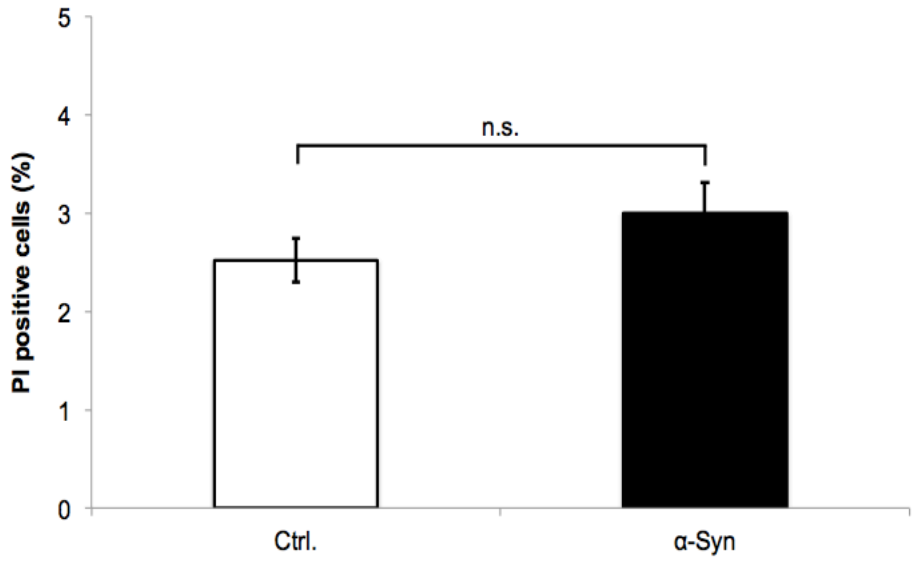

Figure 32: Cell death indicated by flow cytometric quantification of propidium iodide (PI) staining of Pep4p^{GFP} expressing cells with and without co-expression of human α-synuclein (α-Syn). Cell death was analysed after 24h after induction. Means ± s.e.m., n=12; n.s.P>0.05.

Since, α-synuclein cytotoxicity was absent in these Pep4p^{GFP} strains, although α-synuclein expression in these cells was demonstrated, no conclusion about the localization of Pep4p and its alteration by α-synuclein expression could be made.

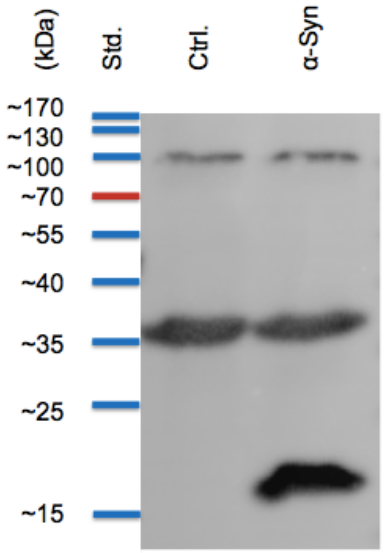

Figure 33: Immunoblot analysis of α-synuclein (α-Syn) expression using antibodies directed against FLAG epitope and against GAPDH as a loading control. Immunoblot was used to detect α-synuclein expression in Pep4p^{GFP} cells.

4. Discussion

4.1. Yeast as model to study Parkinson's disease

Nearly 200 years after its first description, PD pathogenesis still remains enigmatic. Hereditable forms of this disease provided important insights into the molecular basis of PD and helped to identify the protein α-synuclein as a key player in this pathology. α-synuclein became very interesting in PD research, since it was shown to be the major component of the proteinaceous deposits called Lewy bodies, the hallmark of PD. To selectively study the impact of α-synuclein in this pathology, yeast is an ideal model organism, because it fully lacks a nervous system and other proteins, which might be involved in neurodegeneration, but it shares important mechanisms in the clearance of misfolded proteins, which are conserved from yeast to humans.

In this work, heterologous expression of human α-synuclein in *Saccharomyces cerevisiae* was used as a model for PD. α-synuclein expression caused an increase in ROS production and cell death. These effects were already observed in an early phase of expression, which is in line with previous studies [55]. Because of the high cell death rate of nearly 50% already 48 hours after induction, only this early phase of expression was investigated in further experiments.

In aggregate, α-synuclein caused a significant toxic phenotype in yeast cells. Therefore, the created model was used in further experiments to analyse the impact of the yeast ortholog of Cathepsin D, Pep4p, on α-synuclein mediated changes in cell physiology.

4.2. Pep4p alleviated α-synuclein caused cell death

The main aim of this study was to analyse the impact of Pep4p on α-synuclein cytotoxicity, since the role of this protein in PD has been controversially discussed [48, 49]. Therefore, overexpression of Pep4p was performed, which is considered to enhance the vacuolar breakdown as the final stage of autophagy. It is known from aging experiments that the overexpression of the wild type form of Pep4p ($Pep4p^{WT}$) causes an increased lifespan of yeast cells. Also a double point mutation of Pep4p ($Pep4p^{DPM}$), which lacks enzymatic activity, and the propeptide of Pep4p ($Pep4p^{Pro}$) inhibit programmed necrosis [47]. For that reason, the expression of all three variants was performed, to study impacts on α-synuclein cytotoxicity.

A significant reduction of α-synuclein caused ROS production and cell death was observed by expression of $Pep4p^{WT}$ 24 and 48 hours after induction. This clearly indicated a cytoprotective effect of $Pep4p^{WT}$ overexpression Since $Pep4p^{DPM}$ did not cause significant changes, it is likely that reduction of α-synuclein toxicity via $Pep4p^{WT}$ overexpression depends on the enzymatic activity of Pep4p.

Interestingly, $Pep4p^{Pro}$ even enhanced α-synuclein caused cytotoxicity. It was shown in previous studies that overexpression of Pep4p, as well as the overexpression of the propeptide, led to a higher level of spermidine [47]. This metabolite is controversially discussed in PD pathogenesis. While in vitro studies showed an enhancement of α-synuclein aggregation caused by spermidine [65, 66], in vivo studies suggest a reduction of α-synuclein toxicity via a spermidine-mediated induction of autophagy [67]. Therefore, it would be interesting to determine spermidine levels depending on $Pep4p^{WT}$ and $Pep4p^{Pro}$ expression, with and without co-expression of α-synuclein. In this way it can be examined if both constructs are able to increase spermidine levels under this conditions in vivo. A raise of spermidine via $Pep4p^{PRO}$, but decrease through $Pep4p^{WT}$ would point out a negative effect of spermidine on α-synuclein toxicity. If both constructs elevated spermidine levels, which lead to an induction of autophagy, it would be possible that only the expression of $Pep4p^{WT}$ provided enough vacuolar peptidase activity to degrade the toxic protein α-synuclein. By contrast, induction of autophagy in $Pep4p^{PRO}$ expressing cells, mediated by increased spermidine levels, might have

caused autophagic cell death. Therefore, determination of spermidine levels in this experiment might further add to our understanding of the observed cytoprotective effects of Pep4p^{WT} and would shed light on the controversially discussed role of spermidine levels in PD.

Taken together, these findings clearly showed a reduction of α-synuclein-caused ROS production and cell death by Pep4p^{WT} overexpression, which depends on the enzymatic activity of Pep4p.

4.3. Pep4p reduced ROS production and increased survival under respiratory conditions

In this study, Pep4p^{WT} overexpression also led to reduced ROS production caused by α-synuclein. Furthermore, clonogenic survival was determined under respiratory conditions using YPGly plates. Under this condition, cells are forced to aerobic metabolism, which would cumulatively increase ROS production in α-synuclein expressing cells, since this protein was shown to impair mitochondria [22].

Preliminary data from survival plating on YPGly showed significant cell death caused by α-synuclein. Under these respiratory conditions, Pep4p^{WT} expression was sufficient to reduce α-synuclein-cause cell death in such a powerful manner that no significant increase of cell death comparing Pep4p^{WT} expressing cells with and without heterologous expressed α-synuclein could be observed. Thus, Pep4p^{WT} is able to reduce cell death caused by α-synuclein under respiratory conditions, which is likely due to a reduction of ROS production. Interestingly, a tight interplay between mitochondria and the vacuole in acetic acid-induced apoptosis was suggested. In this scenario, the overexpression of Pep4p led to an enhanced degradation of mitochondria [68]. Since α-synuclein cytotoxicity is (at least in part) due to an impairment of mitochondrial function and/or and induction of the mitochondrial pathway of apoptosis [22, 55] it would be interesting to selectively study the influence of Pep4p on mitophagy. This could be done for example by studying the cytoprotective effect of Pep4p^{WT} overexpression on α-synuclein in an Atg11 knockout strain. Since this protein is essential for mitophagy [69], an absence of Pep4p^{WT} caused cytoprotection regarding α-synuclein toxicity in this strain would suggest an essential role of mitophagy in this process.

4.4. α-synuclein oligomers were degraded by Pep4p

Since the shown results suggest an alleviation of cytotoxicity by Pep4p because of its peptidase activity, it was interesting to know, if a reduced amount of α-synuclein could be detectable in co-expressing cells. Especially reductions of α-synuclein oligomers were of interest, as these were shown to be the most toxic form [62]. α-synuclein oligomers could be detected in this study with different molecular weights ranging from approximately 30 to 40 kDa. The most prominent oligomeric band appeared with a molecular weight of 35 kDa, which is considered to be a dimer of α-synuclein. The different molecular weights of the detected bands might be due to diverse posttranslational modifications known for α-synuclein and possible truncations of the C-terminus, which interacts with full-length α-synuclein to accelerate its aggregation [18]. All constituted oligomeric bands of α-synuclein were significantly reduced by $Pep4p^{WT}$ overexpression.

Aggregation of α-synuclein, which forms Lewy bodies as the hallmark of PD, is believed to be the key event in PD pathogenesis. The presented results are further evidence for the hypothesis that especially oligomeric forms of α-synuclein execute cytotoxicity. This is because the overexpression of $Pep4p^{WT}$ led to a reduction of these forms in a proteinase-dependent manner, which was accompanied by a significant decrease of cell death and ROS production.

Interestingly, another study hypothesised an enhanced aggregation of α-synuclein via Pep4p, respectively human Cathepsin D, by increasing the amount of C-terminal truncated forms of α-synuclein [49]. This study used the inhibitor pepstatin to block Cathepsin D activity. But pepstatin is known to inhibit other acid proteases, such as Cathepsin E [70], as well as NF-κB signalling [71], which was shown to be up-regulated in PD [72, 73]. Therefore the observed decline of α-synuclein aggregation cannot be fully linked to Cathepsin D inhibition. However, results in this present work do not only show a degradation of α-synuclein oligomers and a decrease of cell death via Pep4p overexpression, but as discussed later, α-synuclein-caused cell death was significantly higher in Δpep4 strains, in which Pep4p activity is knocked out selectively.

4.5. α-synuclein caused cytoplasmatic acidification

Many neurodegenerative diseases like PD, Alzheimer's disease and Morbus Huntington are caused by protein misfolding, leading to proteinaceous deposits. Another common feature of neurodegeneration is the disruption of pH homeostasis, which is connected to impairments of autophagy [56, 57]. However this event was not described in PD so far. Since $Pep4p^{WT}$ was shown to protect yeast cells from acetic acid-induced apoptosis in a catalytic dependent manner [74] , the next logical step was to analyse influences of α-synuclein on pH homeostasis, and if $Pep4p^{WT}$ was able to prevent possible changes.

By staining cells with Quinacrine, which accumulates in acidic parts of the cell, a cytoplasmatic acidification caused by α-synuclein was demonstrated for the first time. Further it was shown, that $Pep4p^{WT}$, but not $Pep4p^{DPM}$ or $Pep4p^{Pro}$ prevented cells from this pH disruption. Since enhanced α-synuclein aggregation was detectable at lower pH values [11], here shown results provide further evidence for a connection between protein aggregation and cytoplasmatic acidification in PD. By reducing cytoplasmatic acidification, enzymatic active Pep4p inhibited α-synuclein oligomer formation, ROS accumulation and cell death. The exact mechanism by which $Pep4p^{WT}$ alleviated cytoplasmatic acidification remains unclear. However, an enhanced procession of proton pumps in the vacuolar- or plasma membrane through $Pep4p^{WT}$ is unlikely to cause this effect, since an overexpression of Pma1p, Vma1p and Vph2p did not decrease α-synuclein toxicity (data not shown). Another mechanism that can cause the acidification of the cytoplasm is the degradation of the vacuolar membrane, resulting in the release of acidic compounds from the vacuole into the cytosol. As discussed later, this effect was also not observed for α-synuclein in this study.

4.6. Vacuolar morphology changed by α-synuclein and Pep4p

Because Quinacrine stained the acidic parts of yeast cells, vacuoles were observable in cells without α-synuclein expression. In $Pep4p^{WT}$ expressing cells, it seemed that there were more vacuoles in average per cell than in the empty vector control. Because the strong fluorescence signal of the Quinacrine staining did not allow a precise evaluation of this effect, cells were stained with MDY-64, which selectively stains the vacuolar membrane.

As assumed from Quinacrine staining, the MDY-64 staining revealed a morphological change of vacuoles as a result of $Pep4p^{WT}$ expression. These cells had a significant higher number of vacuoles, compared to the empty vector control. Astonishingly, α-synuclein expressing cells also displayed conspicuous vacuolar morphology in form of bigger vacuoles in a lower quantity. In α-synuclein and $Pep4p^{WT}$ co-expressing cells, the phenotype of vacuoles was quite similar to empty vector control cells and no statistically significant changes could be detected.

As cells age, the normal vacuole phenotype proceeds from a higher number of small vacuoles to one big mature vacuole. The vacuolar morphology of α-synuclein expressing cells therefore reflected an older phenotype compared to cells of the empty vector control 16 hours after induction, whereas $Pep4p^{WT}$ somehow kept young vacuolar morphology. The advantage of this high amount of small vacuoles might be a more favourable surface-to-volume ratio for the clearance of damaged and misfolded proteins. The smaller the volume of a vacuole (or any other object) is the bigger is its surface compared to the volume. This means, that with a higher number of smaller vacuoles, a comparatively higher surface is available for reaction. In case of autophagy, this means a higher fusion rate of autophagosomes with the vacuole. Since it is proposed, that α-synuclein causes a block of autophagy [30], the observed vacuolar phenotype would explain the mechanism behind this effect. Because α-synuclein causes big vacuoles in low abundance, this leads to a reduced surface-to-volume ratio, therefore causes a lower fusion rate of autophagosomes with the vacuole.

In this scenario, the autophagic-lysosomal pathway cannot degrade α-synuclein efficiently, which results in aggregation and cell death already after 16 hours. The amount of vacuoles in empty vector control cells was not significantly different to α-synuclein expressing cells 24 hours after induction, but $Pep4p^{WT}$ expressing cells maintained their vacuolar morphology, even in the presence of α-synuclein. This fact further supports the theory of a better surface-to-volume ratio, since $Pep4p^{WT}$ expression significantly reduced cell death caused by α-synuclein 24 and 48 hours after induction.

4.7. α-synuclein did not cause VMP

Lysosomal membrane permeabilization is an event, which can occur in cell death [58]. Because not only a higher rate of dead cells was detected in α-synuclein expressing cells, but also a change of vacuolar morphology and cytoplasmatic acidification, the thought of vacuolar membrane permeabilization (VMP) via α-synuclein stood to reason. Therefore the hypothesis should be tested, if α-synuclein caused VMP, which led to a release of acidic compounds of the vacuole to the cytoplasm as a pre-lethal event.

By incubating cells with FITC-coupled dextrans of different molecular weights, the process of VMP should be detectable via fluorescence microscopy. Since this method was used for the first time in our laboratory, an optimization of the staining protocol was needed. Some steps of the developed staining protocol were essential for the assay to function at all and should therefore be discussed here. Important for the staining was the use of SMD medium, since the uptake of FITC-dextrans is an energy dependent process. But due to autofluorescence caused by the medium, cells were washed with PBS at least three times. By doing so, it was important to put cells immediately on ice after staining, because a rapid reduction of the fluorescence signal was observed when cells were kept on room temperature (possibly through faster degradation of the dextrans in the vacuoles).

A release of the fluorescence signal from the vacuole to the cytosol was not observed in any of the used FITC-coupled dextrans (average molecular weight of 10, 40, 70 and 250 kDa). Therefore it is unlikely, that α-synuclein caused VMP.

A problem in this experiment was the absence of a positive control, especially since this method was not established in our laboratory so far. It is suggested to check the ability of this assay to track VMP, by treating cells with staurosporine, which was shown to induce VMP [58]. However, α-synuclein-caused VMP was not observed in this study and the absence of VMP in α-synuclein caused cell death is not impossible, since VMP and the release of Cathepsin D to the cytosol seem to amplify rather than initiate apoptosis [75].

4.8. Pep4p mislocalization through α-synuclein could not be ruled out

The impact of α-synuclein on vacuolar morphology, as well as the caused cytoplasmatic acidification indicated a disturbance of vacuolar integrity, even though no VMP could be observed. Because the overexpression of $Pep4p^{WT}$ reduced α-synuclein cytotoxicity, the effects of α-synuclein on endogenous expressed Pep4p, as the main vacuolar peptidase, should be explored. By using endogenously GFP-tagged Pep4p expressing cells, the localization of Pep4 was monitored via fluorescence microscopy.

Although Pep4p was localized in the vacuoles with and without α-synuclein expression, it could not be ruled out that α-synuclein led to a mislocalization of Pep4p, because no α-synuclein caused cell death was observed in the used strains. Immunoblots revealed, that α-synuclein was expressed in these cells, thus the absence of toxicity cannot be explained. The used strains were created in a high throughput procedure, so that mistakes in the creation of these strains cannot be excluded. A further sign for damaged strains was a much slower growth of these $Pep4p^{GFP}$ expressing cells.

As discussed below, α-synuclein also caused an enzymatic activity reduction of endogenous expressed Pep4p, which is a hint that Pep4p might be a direct target of α-synuclein. If this would be the case, the GFP-tag possibly reduced interactions of α-synuclein and Pep4p, which protected cells from toxicity. But since a lot of α-synuclein targets are known nowadays, such a protection of Pep4p through the GFP-tag would definitely not inhibit cells from any α-synuclein cytotoxicity. It is therefore strongly recommended to repeat this experiment with a self-created endogenous GFP-tagged Pep4p expressing strain.

4.9. Impacts of α-synuclein on autophagy

The impact of α-synuclein on autophagy is quite controversially discussed. The point mutation A53T of α-synuclein showed an increased rate of cell death via induction of autophagy in neuronal cell culture [35]. Furthermore, wild type α-synuclein, as well as the A53T point mutation led to a raise of cell death through autophagy in a yeast model [36]. On the other hand, the great majority of studies show protective effects of autophagy [31-34]. Data from our lab demonstrated an up-regulation of autophagy, but a block of the autophagic protein breakdown within the vacuoles, which was partly restored by external administration of Ca^{2+} to yeast culture in the moment of induction (unpublished data).

The present work confirmed that α-synuclein caused an induction of autophagy, since the Atg8-GFP/GADPH ratio was higher in α-synuclein expressing cells, which expressed endogenous GFP-tagged Atg8p. Because of a lower free GFP/Atg8p-GFP ratio in these cells, the block of autophagic protein breakdown was also observed.

As discussed above, α-synuclein caused a morphological change of vacuoles, which might result in a worse surface-to-volume ratio. This might be one of the reasons, why autophagic flux was reduced in these cells, leading to the observed accumulation of autophagosomes, and the diffuse GFP signal in the cytoplasm. Since, $Pep4p^{WT}$ led to the opposite phenotype with an increased surface-to-volume ratio, the Atg8-GFP/GAPDH ratio was higher, suggesting an additional up-regulation of autophagy. The fact that the free GFP/Atg8-GFP level was much lower when $Pep4p^{WT}$ was expressed is not very surprising.

The overexpression of this peptidase led to a much higher vacuolar breakdown through the high peptidase activity, which degraded free GFP. These results claim an enhanced autophagy and a release of the α-synuclein caused block of vacuolar degradation via $Pep4p^{WT}$, which might be due to the morphological changes of the vacuoles induced by $Pep4p^{WT}$.

Because the external administration of Ca^{2+} also reversed the block of autophagic flux (shown in previous studies), additive cytoprotective effects observed with addition of 5 mM Ca^{2+} in this work might further enhance the autophagosome fusion with vacuoles. Therefore it would be interesting to repeat this experiment with the administration of Ca^{2+}.

However, there were some severe problems with fluorescence microscopy of Atg8p-GFP strains expressing $Pep4p^{WT}$. The first problem was the vacuolar phenotype, which made it impossible to clearly distinguish between autophagosomes and small vacuoles. Next, the huge amount of vacuoles led to a very strong fluorescence signal. Because all pictures were taken with the same settings and also processed the same way, it was not possible to optimize picture quality for $Pep4p^{WT}$ expressing cells, otherwise other expression types would have been much too dark to recognize anything. Further, pictures were not taken with confocal microscopic techniques, leading to out-of-focus fluorescence. These problems caused a massive loss of information, so that vacuoles were not clearly shown in $Pep4p^{WT}$ expressing cells. Especially the out-of-focus fluorescence led to diffuse fluorescence signal, which falsely seemed to come from the cytosol. But as can be seen in the magnification of presented pictures, $Pep4p^{WT}$ expressing cells that showed a blocked autophagic phenotype had some diffuse vacuolar-like structures inside, whereas this was not seen in α-synuclein expressing cells with a blocked autophagic phenotype. Therefore it is considered, that these quite similar looking cells presented two completely different phenotypes: α-synuclein expressing cells showed a block of autophagic flux, leading to an accumulation of Atg8-GFP in the cytosol. $Pep4p^{WT}$ expressing cells displayed a young vacuolar phenotype, insufficiently resolved because of inadequate microscopy techniques used, which looked like diffuse fluorescence coming from the cytosol.

Because of the problems with fluorescence microscopy in this experiment, pictures were not quantified for $Pep4p^{WT}$ expressing cells. It is highly recommended to repeat this experiment using confocal microscopy. Furthermore, different ATG knockout strains could be used for the investigation of the cytoprotective effects of $Pep4p^{WT}$. If $Pep4p^{WT}$ does not reduce α-synuclein-caused cell death in these strains, the alleviation is very likely to depend on autophagy.

4.10. The connection between Ca^{2+} and Pep4p in α-synuclein cytotoxicity

In the last few years the role of Ca^{2+}-homeostasis in α-synuclein toxicity was intensively studied in our laboratory. Disturbances of intracellular Ca^{2+} levels, mediated by Pmr1p [24] were observed, as well as a reduction of α-synuclein toxicity by administration of Ca^{2+} to yeast culture (unpublished data).

In the present work, a connection between the cytoprotective effects of Ca^{2+} administration and $Pep4p^{WT}$ overexpression was analysed. The additive effects of these two approaches were demonstrated, as well as the fact that protective effect of Ca^{2+} depended on Pep4p expression, since no reduction of α-synuclein toxicity via Ca^{2+} was observed in Δpep4 strains. An enhancement of α-synuclein-caused cell death and ROS production was revealed in cells lacking Pep4p expression. This indicated that endogenous expressed Pep4p had an active role to reduce pathophysiological changes in cells, which express α-synuclein.

As shown in previous experiments, α-synuclein decreased enzymatic activity of endogenous expressed Pep4p, whereas addition of Ca^{2+} to yeast cultures did not only restore activity, but significantly enhanced activity compared to empty vector control cells. Together, these results suggest a Ca^{2+}/Pep4p connection, which is sufficient to reduce α-synuclein cytotoxicity. This connection is likely to consist in a more efficient autophagosome-vacuole fusion, mediated by Ca^{2+}-signalling and the higher surface-to-volume ratio due to Pep4p expression, as well as an increased vacuolar breakdown because of the higher peptidase activity caused via Pep4p overexpression.

For a better understanding of the peptidase activity enhancement, it would be interesting, if Ca^{2+} could also increase Pep4p enzymatic activity when added to the protein lysate. This would indicate direct interactions between Pep4p and Ca^{2+}. But more likely, there is a complex signalling involved in this process. One possibility is the plasma membrane ATP-binding cassette transporter Pdr5p, which might be involved in Ca^{2+} homeostasis in a calcineurin and Pep4p dependent manner [76]. This protein might be particularly interesting, since Ca^{2+} cytoprotective effects seem to depend on calcineurin (unpublished data) and on Pep4p, as shown in this work.

4.11. Summary

This work gave new insights into α-synuclein pathophysiology. Results of all findings are summed up graphically in Figure 34. In addition to an increased cell death and ROS production, α-synuclein also caused cytoplasmatic acidification, which might enhance the formation of toxic oligomeric forms. All of these toxic effects were alleviated by the overexpression of the vacuolar peptidase Pep4p. It was shown that this reduction of cytotoxicity depended on the protease activity of this enzyme. Since α-synuclein decreased the activity of endogenous expressed Pep4p and a higher α-synuclein caused toxicity was observed in Δpep4 strains, it is considered, that Pep4p is involved in cytoprotective responses of cells against α-synuclein damages.

Further α-synuclein led to morphological changes of vacuoles, which reflects a faster maturation process of vacuoles, leading to a lower surface-to-volume ratio. α-synuclein caused an induction of autophagy, but a block of vacuolar breakdown, which resulted in an accumulation of autophagosomes. An overexpression of Pep4p led to a high quantity of small vacuoles in cells, causing a high surface-to-volume ratio, which might be involved in a release of the autophagosome-vacuole fusion block. Furthermore, Pep4p overexpression led to an enhanced peptidase activity in the vacuole. Because of the resulting enhancement of the vacuolar breakdown, Pep4p overexpression led to a reduction of toxic α-synuclein oligomers.

The external administration of Ca^{2+} to yeast cells mediated a reduction of α-synuclein-caused ROS production and cell death, which depends on the expression of Pep4p. Ca^{2+} treatment caused an increase of Pep4p activity, and by simultaneous Pep4p overexpression and Ca^{2+} administration, additive cytoprotective effects against α-synuclein toxicity were observed.

These results reveal a cytoprotective role of Pep4p in PD and a so far unknown Ca^{2+}/Pep4p connection, which might improve autophagy-mediated clearance of α-synuclein oligomers, leading to a reduced cytotoxicity. Underlying pathways of this connection might be interesting for the development of new therapies targeting α-synuclein toxicity in PD.

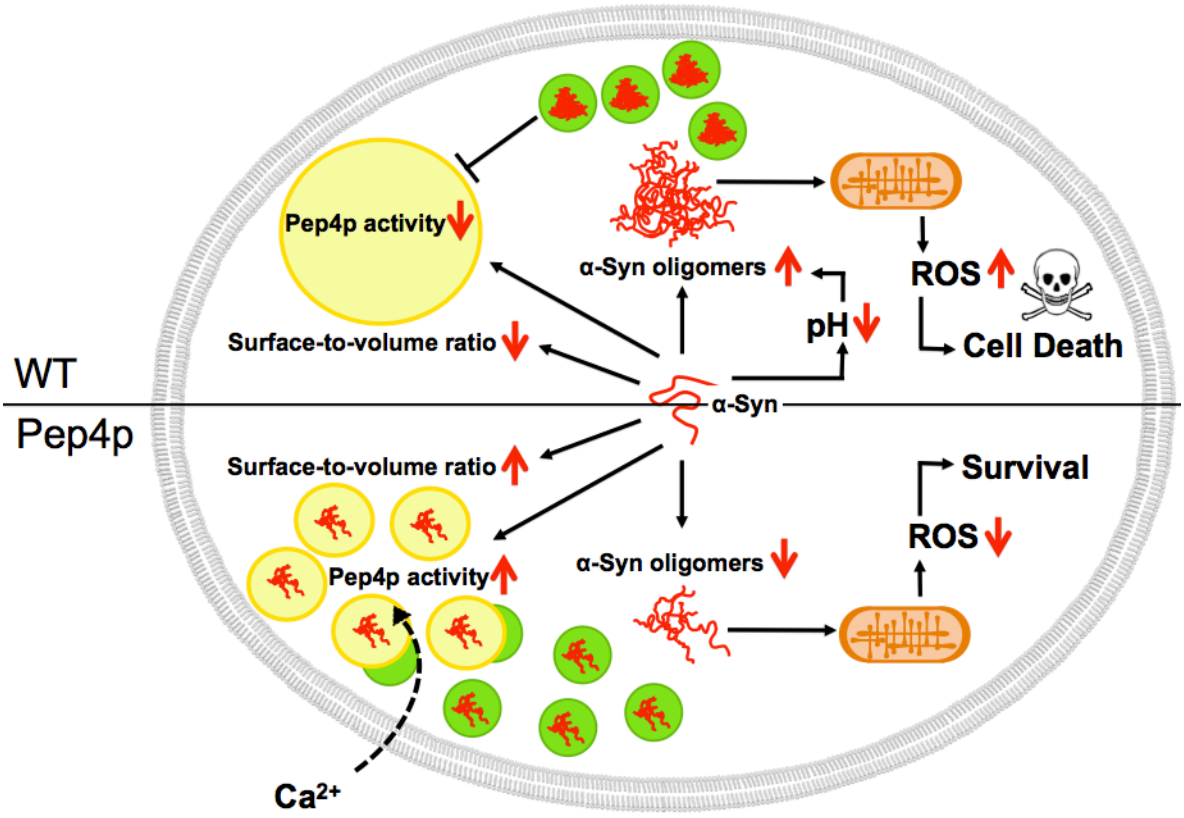

Figure 34: Overview of hypothesised mechanisms of α-synuclein toxicity and Pep4p cytoprotection. See text for description. Figure legend: yellow: vacuoles; green: autophagosomes; orange: mitochondria; WT: wild type cells with α-synuclein expression; Pep4p: $Pep4p^{WT}$ and α-synuclein co-expressing cells

4.12. Outlook

Interestingly, it was observed that the overexpression of $Pep4p^{Pro}$ enhanced α-synuclein toxicity, but $Pep4p^{Pro}$ overexpression was reported to increase spermidine levels [47]. Because spermidine was shown to reduce α-synuclein toxicity [67], it would be interesting to determine spermidine levels in $Pep4p^{WT}$ and $Pep4p^{PRO}$ expressing cells, to further investigated the role of this metabolite in cytoprotective mechanisms.

Because of artefacts in fluorescence microscopy pictures of Atg8p-GFP expressing cells, the results of $Pep4p^{WT}$ overexpression were not precisely evaluable. Here, confocal microscopy might do the trick. In addition, $Pep4p^{WT}$ cytoprotection should be examined in different ATG knockout strains, to evaluate a possible dependence of reduced α-synuclein toxicity on autophagy.

The absence of α-synuclein-caused cell death in Pep4p localization experiments, allowed no sure statement concerning α-synuclein mediated Pep4p mislocalization. This experiment should be repeated with a self-created endogenous GPF-tagged Pep4p expressing strain. Further, the demonstrated absence of vacuolar membrane permeabilization should be checked using a positive control to prove the functionality of the assay.

Very interesting is the remaining question about the underlying pathways of Ca^{2+}/Pep4p connection in reduction of α-synuclein-caused cell death. Here, a direct influence of Ca^{2+} on Pep4p activity should be excluded by adding of Ca^{2+} to protein lysate of Pep4p overexpressing cells. If a direct interaction causes the alteration of enzymatic activity, it should be observable in this assy.

It is likely, that this connection consists of a more sophisticated regulation. To screen for possible participants, one easy method would be immunoblotting with antibodies against assumed proteins to detect alterations of their expression on protein level. For example Pdr5p should be considered, since it is involved in regulation of Ca^{2+} sensitivity together with Pep4p [76]. Other promising candidates in this pathway might be calcineurin, calmodulin and Cmk1p.

5. Supplementary Material

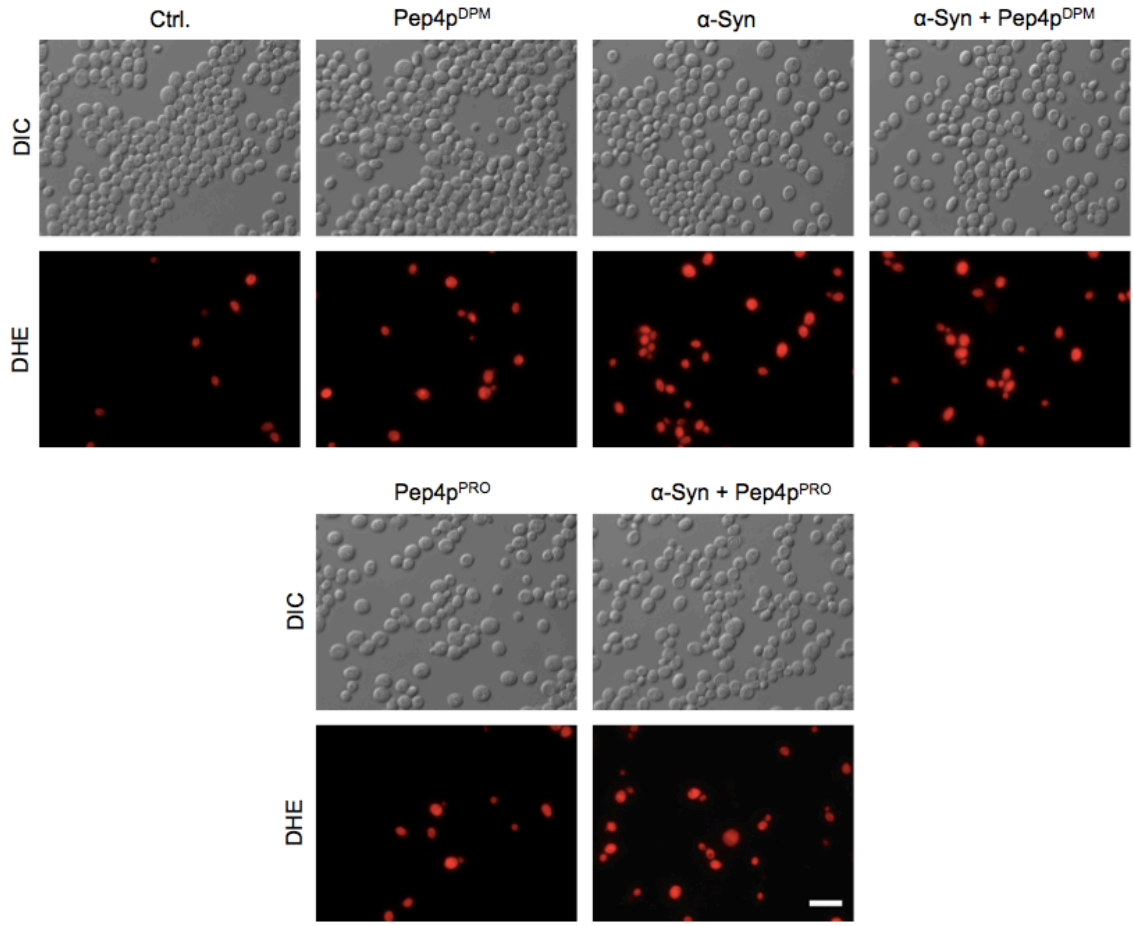

S 1: Fluorescence microscopic sample pictures of DHE stained wild type cells (Ctrl.), double point mutation of Pep4p (Pep4p^{DPM}) and propeptide of Pep4p (Pep4p^{PRO}) expressing cells with and without co-expression of human α-synuclein (α-Syn) 24 hours after induction. After flow cytometric quantification of DHE to Eth conversion, cells were pooled and analysed by fluorescence microscopy to visualize determined ROS accumulation. Scale bar represents 10 µm.

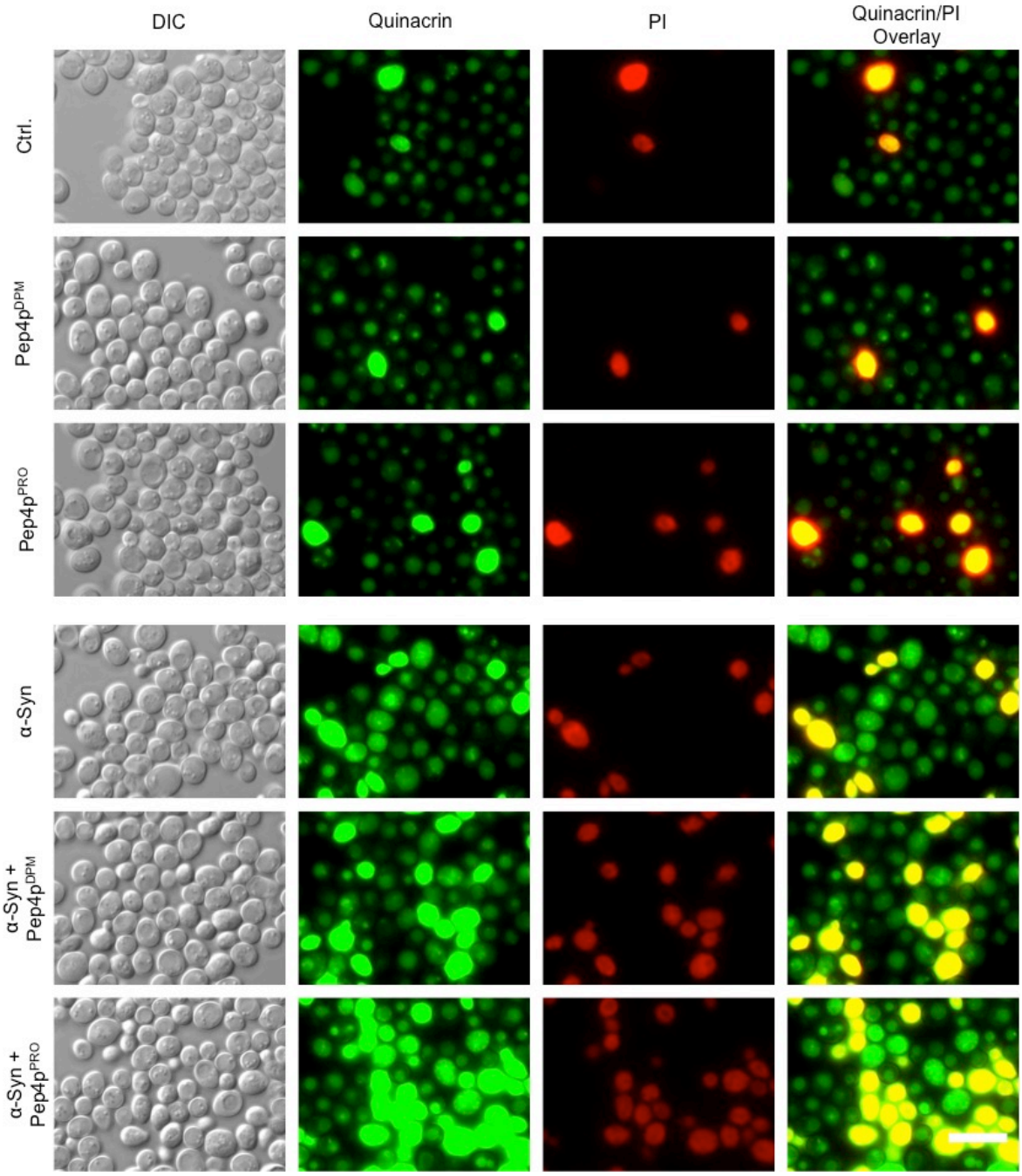

S 2: Fluorescence microscopic sample pictures of Quinacrine stained wild type cells (Ctrl.), double point mutation of Pep4p (Pep4p^{DPM}) and propeptide of Pep4p (Pep4p^{PRO}) expressing cells with and without co-expression of human α-synuclein (α-Syn) 24 hours after induction. Quinacrine staining was used to indicate acidic parts of the cells. Scale bar represents 10 µm.

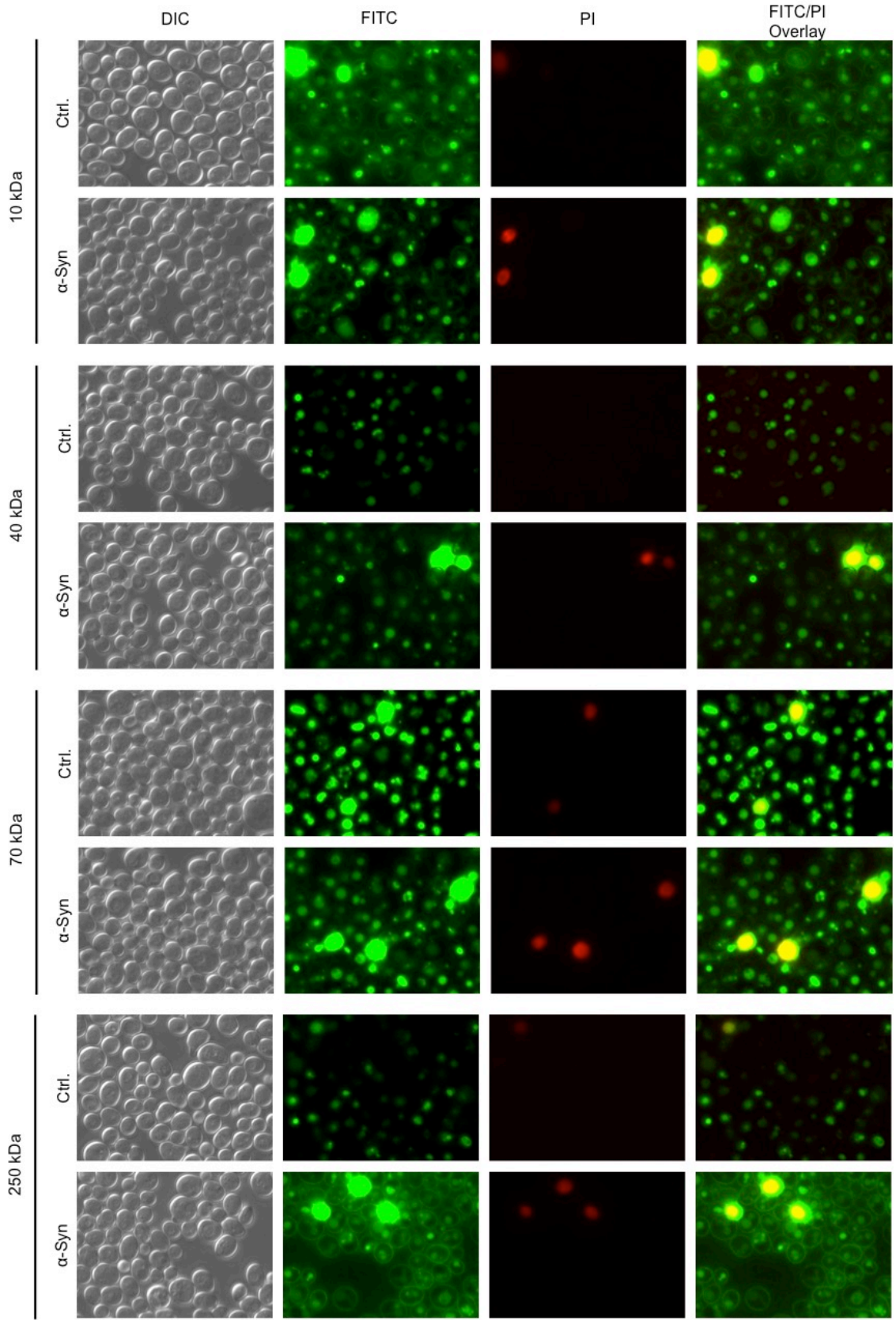

S 3: Fluorescence microscopic sample pictures of wild type cells (Ctrl.) with and without co-expression of human α-synuclein (α-Syn) incubated with FITC-coupled dextrans to detect vacuolar membrane permeabilization (VMP). Declared molecular weight refers to the average molecular weight of different dextrans. Scale bar represents 10 µm.

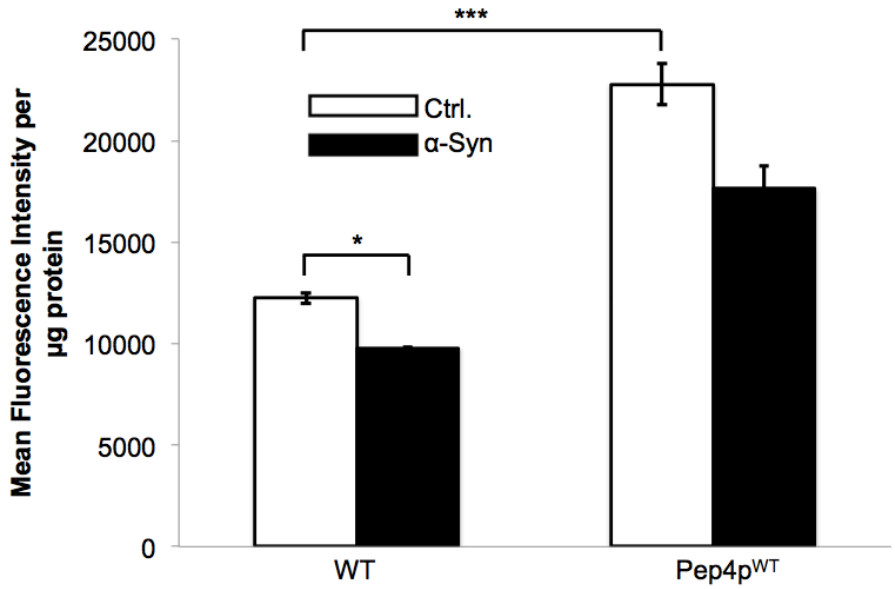

S 4: Quantification of Pep4p activity in wild type cells (WT) and Pep4p (Pep4p^{WT}) expressing cells, with and without co-expression of human α-synuclein (α-Syn) 16 hours after induction. Means ± s.e.m., n=3. ***P<0.001; *P<0.05

6. References

1. Noyce AJ, Bestwick JP, Silveira‐Moriyama L, Hawkes CH, Giovannoni G, Lees AJ, Schrag A (2012). Meta‐analysis of early nonmotor features and risk factors for parkinson disease. Ann Neurol. **72:**893-901.

2. Pringsheim T, Jette N, Frolkis A, Steeves TD (2014). The prevalence of parkinson's disease: A systematic review and meta‐analysis. Movement Disorders. **29:**1583-1590.

3. Spillantini MG, Schmidt ML, Lee VM, Trojanowski JQ, Jakes R, Goedert M (1997). A-synuclein in lewy bodies. Nature. **388:**839-840.

4. Spillantini MG, Crowther RA, Jakes R, Hasegawa M, Goedert M (1998). Alpha-synuclein in filamentous inclusions of lewy bodies from parkinson's disease and dementia with lewy bodies. Proc Natl Acad Sci U S A. **95:**6469-6473.

5. Burre J, Sharma M, Tsetsenis T, Buchman V, Etherton MR, Sudhof TC (2010). Alpha-synuclein promotes SNARE-complex assembly in vivo and in vitro. Science. **329:**1663-1667.

6. Polymeropoulos MH, Lavedan C, Leroy E, Ide SE, Dehejia A, Dutra A, Pike B, Root H, Rubenstein J, Boyer R, Stenroos ES, Chandrasekharappa S, Athanassiadou A, Papapetropoulos T, Johnson WG, Lazzarini AM, Duvoisin RC, Di Iorio G, Golbe LI, Nussbaum RL (1997). Mutation in the alpha-synuclein gene identified in families with parkinson's disease. Science. **276:**2045-2047.

7. Zarranz JJ, Alegre J, Gómez‐Esteban JC, Lezcano E, Ros R, Ampuero I, Vidal L, Hoenicka J, Rodriguez O, Atarés B (2004). The new mutation, E46K, of α‐synuclein causes parkinson and lewy body dementia. Ann Neurol. **55:**164-173.

8. Krüger R, Kuhn W, Müller T, Woitalla D, Graeber M, Kösel S, Przuntek H, Epplen JT, Schols L, Riess O (1998). AlaSOPro mutation in the gene encoding α-synuclein in parkinson's disease. Nat Genet. **18:**106-108.

9. Singleton AB, Farrer M, Johnson J, Singleton A, Hague S, Kachergus J, Hulihan M, Peuralinna T, Dutra A, Nussbaum R, Lincoln S, Crawley A, Hanson M, Maraganore D, Adler C, Cookson MR, Muenter M, Baptista M, Miller D, Blancato J, Hardy J, Gwinn-Hardy K (2003). Alpha-synuclein locus triplication causes parkinson's disease. Science. **302:**841.

10. Farrer M, Kachergus J, Forno L, Lincoln S, Wang D, Hulihan M, Maraganore D, Gwinn‐Hardy K, Wszolek Z, Dickson D (2004). Comparison of kindreds with parkinsonism and α‐synuclein genomic multiplications. Ann Neurol. **55:**174-179.

11. Uversky VN, Li J, Fink AL (2001). Evidence for a partially folded intermediate in alpha-synuclein fibril formation. J Biol Chem. **276:**10737-10744.

12. Fujiwara H, Hasegawa M, Dohmae N, Kawashima A, Masliah E, Goldberg MS, Shen J, Takio K, Iwatsubo T (2002). A-synuclein is phosphorylated in synucleinopathy lesions. Nat Cell Biol. **4:**160-164.

13. Smith WW, Margolis RL, Li X, Troncoso JC, Lee MK, Dawson VL, Dawson TM, Iwatsubo T, Ross CA (2005). Alpha-synuclein phosphorylation enhances eosinophilic cytoplasmic inclusion formation in SH-SY5Y cells. J Neurosci. **25:**5544-5552.

14. Paleologou KE, Oueslati A, Shakked G, Rospigliosi CC, Kim HY, Lamberto GR, Fernandez CO, Schmid A, Chegini F, Gai WP, Chiappe D, Moniatte M, Schneider BL, Aebischer P, Eliezer D, Zweckstetter M, Masliah E, Lashuel HA (2010). Phosphorylation at S87 is enhanced in synucleinopathies, inhibits alpha-synuclein oligomerization, and influences synuclein-membrane interactions. J Neurosci. **30:**3184-3198.

15. Haywood AF, Staveley BE (2004). Parkin counteracts symptoms in a drosophila model of parkinson's disease. BMC Neurosci. **5:**14.

16. Li W, West N, Colla E, Pletnikova O, Troncoso JC, Marsh L, Dawson TM, Jakala P, Hartmann T, Price DL, Lee MK (2005). Aggregation promoting C-terminal truncation of alpha-synuclein is a normal cellular process and is enhanced by the familial parkinson's disease-linked mutations. Proc Natl Acad Sci U S A. **102:**2162-2167.

17. Ulusoy A, Febbraro F, Jensen PH, Kirik D, Romero-Ramos M (2010). Co-expression of c-terminal truncated alpha-synuclein enhances full-length alpha-synuclein-induced pathology. Eur J Neurosci. **32:**409-422.

18. Breydo L, Wu JW, Uversky VN (2012). A-synuclein misfolding and parkinson's disease. Biochimica et Biophysica Acta (BBA)-Molecular Basis of Disease. **1822:**261-285.

19. Auluck PK, Caraveo G, Lindquist S (2010). A-synuclein: Membrane interactions and toxicity in parkinson's disease. Annu Rev Cell Dev Biol. **26:**211-233.

20. Van Rooijen BD, Claessens MM, Subramaniam V (2010). Membrane permeabilization by oligomeric α-synuclein: In search of the mechanism.

21. Cooper AA, Gitler AD, Cashikar A, Haynes CM, Hill KJ, Bhullar B, Liu K, Xu K, Strathearn KE, Liu F, Cao S, Caldwell KA, Caldwell GA, Marsischky G, Kolodner RD, Labaer J, Rochet JC, Bonini NM, Lindquist S (2006). Alpha-synuclein blocks ER-golgi traffic and Rab1 rescues neuron loss in parkinson's models. Science. **313:**324-328.

22. Buttner S, Bitto A, Ring J, Augsten M, Zabrocki P, Eisenberg T, Jungwirth H, Hutter S, Carmona-Gutierrez D, Kroemer G, Winderickx J, Madeo F (2008). Functional mitochondria are required for alpha-synuclein toxicity in aging yeast. J Biol Chem. **283:**7554-7560.

23. Chung KK, Dawson VL, Dawson TM (2001). The role of the ubiquitin-proteasomal pathway in parkinson's disease and other neurodegenerative disorders. Trends Neurosci. **24:**S7-S14.

24. Büttner S, Faes L, Reichelt W, Broeskamp F, Habernig L, Benke S, Kourtis N, Ruli D, Carmona-Gutierrez D, Eisenberg T (2013). The Ca2+/Mn2+ ion-pump PMR1 links elevation of cytosolic Ca2+ levels to α-synuclein toxicity in parkinson's disease models. Cell Death & Differentiation. **20:**465-477.

25. Winslow AR, Chen CW, Corrochano S, Acevedo-Arozena A, Gordon DE, Peden AA, Lichtenberg M, Menzies FM, Ravikumar B, Imarisio S, Brown S, O'Kane CJ, Rubinsztein DC (2010). Alpha-synuclein impairs macroautophagy: Implications for parkinson's disease. J Cell Biol. **190:**1023-1037.

26. Dice JF (2007). Chaperone-mediated autophagy. Autophagy. **3:**295-299.

27. Wang CW, Klionsky DJ (2003). The molecular mechanism of autophagy. Mol Med. **9:**65-76.

28. Feng Y, He D, Yao Z, Klionsky DJ (2014). The machinery of macroautophagy. Cell Res. **24:**24-41.

29. Anglade P, Vyas S, Javoy-Agid F, Herrero M, Michel P, Marquez J, Mouatt-Prigent A, Ruberg M, Hirsch E, Agid Y (1997). Apoptosis and autophagy in nigral neurons of patients with parkinson's disease. Histol Histopathol. **12:**25-32.

30. Spencer B, Potkar R, Trejo M, Rockenstein E, Patrick C, Gindi R, Adame A, Wyss-Coray T, Masliah E (2009). Beclin 1 gene transfer activates autophagy and ameliorates the neurodegenerative pathology in alpha-synuclein models of parkinson's and lewy body diseases. J Neurosci. **29:**13578-13588.

31. Chen L, Song J, Lu J, Yuan Z, Liu L, Durairajan SSK, Li M (2014). Corynoxine, a natural autophagy enhancer, promotes the clearance of alpha-synuclein via akt/mTOR pathway. Journal of Neuroimmune Pharmacology. **9:**380-387.

32. Jiang T, Zhang Y, Zhou H, Wang H, Tian L, Liu J, Ding J, Chen S (2013). Curcumin ameliorates the neurodegenerative pathology in A53T α-synuclein cell model of parkinson's disease through the downregulation of mTOR/p70S6K signaling and the recovery of macroautophagy. Journal of NeuroImmune Pharmacology. **8:**356-369.

33. Park HJ, Shin JY, Kim HN, Oh SH, Lee PH (2014). Neuroprotective effects of mesenchymal stem cells through autophagy modulation in a parkinsonian model. Neurobiol Aging. **35:**1920-1928.

34. Steele JW, Ju S, Lachenmayer ML, Liken J, Stock A, Kim SH, Delgado LM, Alfaro IE, Bernales S, Verdile G (2013). Latrepirdine stimulates autophagy and reduces accumulation of α-synuclein in cells and in mouse brain. Mol Psychiatry. **18:**882-888.

35. Choubey V, Safiulina D, Vaarmann A, Cagalinec M, Wareski P, Kuum M, Zharkovsky A, Kaasik A (2011). Mutant A53T alpha-synuclein induces neuronal death by increasing mitochondrial autophagy. J Biol Chem. **286:**10814-10824.

36. Sampaio-Marques B, Felgueiras C, Silva A, Rodrigues M, Tenreiro S, Franssens V, Reichert AS, Outeiro TF, Winderickx J, Ludovico P (2012). SNCA (α-synuclein)-induced toxicity in yeast cells is dependent on Sir2-mediated mitophagy. Autophagy. **8:**1494-1509.

37. Kandel E (1981). Calcium and the control of synaptic strength by learning. Nature.

38. Mayford M, Wang J, Kandel ER, O'Dell TJ (1995). CaMKII regulates the frequency-response function of hippocampal synapses for the production of both LTD and LTP. Cell. **81:**891-904.

39. Sattler R, Tymianski M (2000). Molecular mechanisms of calcium-dependent excitotoxicity. Journal of molecular medicine. **78:**3-13.

40. Orrenius S, Zhivotovsky B, Nicotera P (2003). Regulation of cell death: The calcium–apoptosis link. Nature reviews Molecular cell biology. **4:**552-565.

41. Adamczyk A, Strosznajder JB (2006). Alpha-synuclein potentiates Ca2+ influx through voltage-dependent Ca2+ channels. Neuroreport. **17:**1883-1886.

42. Lowe R, Pountney DL, Jensen PH, Gai WP, Voelcker NH (2004). Calcium (II) selectively induces α-synuclein annular oligomers via interaction with the c-terminal domain. Protein science. **13:**3245-3252.

43. Dehay B, Bove J, Rodriguez-Muela N, Perier C, Recasens A, Boya P, Vila M (2010). Pathogenic lysosomal depletion in parkinson's disease. J Neurosci. **30:**12535-12544.

44. Vila M, Bové J, Dehay B, Rodríguez-Muela N, Boya P (2011). Lysosomal membrane permeabilization in parkinson disease. Autophagy. **7:**98-100.

45. Benes P, Vetvicka V, Fusek M (2008). Cathepsin d—many functions of one aspartic protease. Crit Rev Oncol. **68:**12-28.

46. Parr CL, Keates RA, Bryksa BC, Ogawa M, Yada RY (2007). The structure and function of saccharomyces cerevisiae proteinase A. Yeast. **24:**467-480.

47. Carmona-Gutierrez D, Bauer M, Ring J, Knauer H, Eisenberg T, Büttner S, Ruckenstuhl C, Reisenbichler A, Magnes C, Rechberger G (2011). The propeptide of yeast cathepsin D inhibits programmed necrosis. Cell death & disease. **2:**e161.

48. Qiao L, Hamamichi S, Caldwell KA, Caldwell GA, Yacoubian TA, Wilson S, Xie ZL, Speake LD, Parks R, Crabtree D, Liang Q, Crimmins S, Schneider L, Uchiyama Y, Iwatsubo T, Zhou Y, Peng L, Lu Y, Standaert DG, Walls KC, Shacka JJ, Roth KA, Zhang J (2008). Lysosomal enzyme cathepsin D protects against alpha-synuclein aggregation and toxicity. Mol Brain. **1:**17-6606-1-17.

49. Cullen V, Lindfors M, Ng J, Paetau A, Swinton E, Kolodziej P, Boston H, Saftig P, Woulfe J, Feany MB (2009). Cathepsin D expression level affects alpha-synuclein processing, aggregation, and toxicity in vivo. Mol Brain. **2:**1756-6606.

50. Takahashi M, Ko L, Kulathingal J, Jiang P, Sevlever D, Yen SC (2007). Oxidative stress‐induced phosphorylation, degradation and aggregation of α‐synuclein are linked to upregulated CK2 and cathepsin D. Eur J Neurosci. **26:**863-874.

51. Outeiro TF, Lindquist S (2003). Yeast cells provide insight into alpha-synuclein biology and pathobiology. Science. **302:**1772-1775.

52. Zabrocki P, Pellens K, Vanhelmont T, Vandebroek T, Griffioen G, Wera S, Van Leuven F, Winderickx J (2005). Characterization of α‐synuclein aggregation and synergistic toxicity with protein tau in yeast. Febs Journal. **272:**1386-1400.

53. Eisenberg T, Schroeder S, Andryushkova A, Pendl T, Küttner V, Bhukel A, Mariño G, Pietrocola F, Harger A, Zimmermann A (2014). Nucleocytosolic depletion of the energy metabolite acetyl-coenzyme a stimulates autophagy and prolongs lifespan. Cell metabolism. **19:**431-444.

54. Gietz RD, Woods RA (2002). Transformation of yeast by lithium acetate/single-stranded carrier DNA/polyethylene glycol method. Meth Enzymol. **350:**87-96.

55. Buttner S, Habernig L, Broeskamp F, Ruli D, Vogtle FN, Vlachos M, Macchi F, Kuttner V, Carmona-Gutierrez D, Eisenberg T, Ring J, Markaki M, Taskin AA, Benke S, Ruckenstuhl C, Braun R, Van den Haute C, Bammens T, van der Perren A, Frohlich KU, Winderickx J, Kroemer G, Baekelandt V, Tavernarakis N, Kovacs GG, Dengjel J, Meisinger C, Sigrist SJ, Madeo F (2013). Endonuclease G mediates alpha-synuclein cytotoxicity during parkinson's disease. EMBO J. **32:**3041-3054.

56. Wolfe DM, Lee J, Kumar A, Lee S, Orenstein SJ, Nixon RA (2013). Autophagy failure in alzheimer's disease and the role of defective lysosomal acidification. Eur J Neurosci. **37:**1949-1961.

57. Syntichaki P, Samara C, Tavernarakis N (2005). The vacuolar H -ATPase mediates intracellular acidification required for neurodegeneration in C. elegans. Current Biology. **15:**1249-1254.

58. Boya P, Kroemer G (2008). Lysosomal membrane permeabilization in cell death. Oncogene. **27:**6434-6451.

59. Makarow M, Nevalainen LT (1987). Transport of a fluorescent macromolecule via endosomes to the vacuole in saccharomyces cerevisiae. J Cell Biol. **104:**67-75.

60. Baba M, Nakajo S, Tu PH, Tomita T, Nakaya K, Lee VM, Trojanowski JQ, Iwatsubo T (1998). Aggregation of alpha-synuclein in lewy bodies of sporadic parkinson's disease and dementia with lewy bodies. Am J Pathol. **152:**879-884.

61. Spinelli KJ, Taylor JK, Osterberg VR, Churchill MJ, Pollock E, Moore C, Meshul CK, Unni VK (2014). Presynaptic alpha-synuclein aggregation in a mouse model of parkinson's disease. J Neurosci. **34:**2037-2050.

62. Winner B, Jappelli R, Maji SK, Desplats PA, Boyer L, Aigner S, Hetzer C, Loher T, Vilar M, Campioni S, Tzitzilonis C, Soragni A, Jessberger S, Mira H, Consiglio A, Pham E, Masliah E, Gage FH, Riek R (2011). In vivo demonstration that alpha-synuclein oligomers are toxic. Proc Natl Acad Sci U S A. **108:**4194-4199.

63. Winslow AR, Rubinsztein DC (2011). The parkinson disease protein α-synuclein inhibits autophagy. Autophagy. **7:**.

64. Harr MW, Distelhorst CW (2010). Apoptosis and autophagy: Decoding calcium signals that mediate life or death. Cold Spring Harb Perspect Biol. **2:**a005579.

65. Antony T, Hoyer W, Cherny D, Heim G, Jovin TM, Subramaniam V (2003). Cellular polyamines promote the aggregation of alpha-synuclein. J Biol Chem. **278:**3235-3240.

66. Krasnoslobodtsev AV, Peng J, Asiago JM, Hindupur J, Rochet J, Lyubchenko YL (2012). Effect of spermidine on misfolding and interactions of alpha-synuclein. PloS one. **7:**e38099.

67. Büttner S, Broeskamp F, Sommer C, Markaki M, Habernig L, Alavian-Ghavanini A, Carmona-Gutierrez D, Eisenberg T, Michael E, Kroemer G (2014). Spermidine protects against α-synuclein neurotoxicity. Cell Cycle. **13:**3903-3908.

68. Pereira C, Chaves S, Alves S, Salin B, Camougrand N, Manon S, Sousa MJ, Côrte‐Real M (2010). Mitochondrial degradation in acetic acid‐induced yeast apoptosis: The role of Pep4 and the ADP/ATP carrier. Mol Microbiol. **76:**1398-1410.

69. Kanki T, Klionsky DJ (2008). Mitophagy in yeast occurs through a selective mechanism. J Biol Chem. **283:**32386-32393.

70. Barrett AJ, Dingle JT (1972). The inhibition of tissue acid proteinases by pepstatin. Biochem J. **127:**439-441.

71. Yoshida H, Okamoto K, Iwamoto T, Sakai E, Kanaoka K, Hu JP, Shibata M, Hotokezaka H, Nishishita K, Mizuno A, Kato Y (2006). Pepstatin A, an aspartic proteinase inhibitor, suppresses RANKL-induced osteoclast differentiation. J Biochem. **139:**583-590.

72. Hunot S, Brugg B, Ricard D, Michel PP, Muriel MP, Ruberg M, Faucheux BA, Agid Y, Hirsch EC (1997). Nuclear translocation of NF-kappaB is increased in dopaminergic neurons of patients with parkinson disease. Proc Natl Acad Sci U S A. **94:**7531-7536.

73. Mogi M, Kondo T, Mizuno Y, Nagatsu T (2007). p53 protein, interferon-γ, and NF-κB levels are elevated in the parkinsonian brain. Neurosci Lett. **414:**94-97.

74. Pereira H, Azevedo F, Rego A, Sousa MJ, Chaves SR, Côrte-Real M (2013). The protective role of yeast cathepsin D in acetic acid-induced apoptosis depends on ANT (Aac2p) but not on the voltage-dependent channel (Por1p). FEBS Lett. **587:**200-205.

75. Oberle C, Huai J, Reinheckel T, Tacke M, Rassner M, Ekert PG, Buellesbach J, Borner C (2010). Lysosomal membrane permeabilization and cathepsin release is a bax/bak-dependent, amplifying event of apoptosis in fibroblasts and monocytes. Cell Death & Differentiation. **17:**1167-1178.

76. Tutulan-Cunita AC, Ohnishi T, Mizunuma M, Hirata D, Miyakawa T (2005). Involvement of saccharomyces cerevisiae Pdr5p ATP-binding cassette transporter in calcium homeostasis. Biosci Biotechnol Biochem. **69:**857-860.

7. Appendix: Curriculum Vitae

PERSONAL INFORMATION

Name:	Andreas Aufschnaiter
Born:	02.12.1988 in Kitzbühel, Austria
Address:	Heinrichstraße 112e, A-8010 Graz, Austria
E-mail:	andreas.aufschnaiter@edu.uni-graz.at
Telephone (private):	+43 660 47 929 43

EDUCATION

08/2015 (planned)	**PhD Thesis** Institute of Molecular Biosciences "Dysregulation of autophagy by LRRK2 and α-synuclein in Parkinson's disease models" Supervisor: Sabrina Büttner
08/2015 (planned)	**PhD Programme in Molecular Biology and Biochemistry** Institute of Molecular Biosciences, University of Graz
06/2015 – 07/2015	**Master's Thesis** Institute of Molecular Biosciences, University of Graz „Cathepsin D alleviates α-synuclein cytotoxicity and vacuolar acidification in a yeast model for Parkinson's disease" Supervisor: Sabrina Büttner
10/2013 – 07/2015	**Master's Programme in Biochemistry and Molecular Biomedicine** Institute of Molecular Biosciences, University of Graz
10/2011 - ongoing	**Diploma Studies in Human Medicine** Medical University of Graz, Austria
10/2010 – 07/2013	**Bachelor's Programme Molecular Biology** University of Graz, Austria

ADDITIONAL PRACTICAL EXPERIENCE

Summer 2014	Project Laboratory work Institute of Molecular Biosciences, University of Graz „α-synuclein disrupts cellular pH Homeostasis and Vacuolar Acidification" Supervisor: Sabrina Büttner
Summer 2013	Clinical elective in Neurology Hospital St. John of God Graz-Eggenberg, Austria
Summer 2012	Clinical elective in Internal Medicine Academic teaching hospital St. Johann in Tirol, Austria
Summer 2011	Clinical elective in Surgery Academic teaching hospital St. Johann in Tirol, Austria
Summer 2010	Internship in the area Quality Management in Healthcare Gebro Pharma, Fieberbrunn, Austria

Career related Activities

2015	Organizing Committee 4th Meeting of the 7. Faculty University of Graz, Austria

SKILLS

Languages:	German: native speaker; English: fluent
Computer skills:	Windows and Mac OS X: excellent MS Office: excellent; Software for FACS analysis (BD FACSDivia): excellent Software for Microscopy and image processing (Fiji, ImageJ, MetaMorph): excellent Programming knowledge (C/C++): good
Others:	Qualityaustria certificate in quality management and applied Statistics Qualityaustria certificate in quality engineering